



HAL
open science

Temporal approaches of historical extreme storm events based on sedimentological archives

Pierre Pouzet, Mohamed Maanan

► **To cite this version:**

Pierre Pouzet, Mohamed Maanan. Temporal approaches of historical extreme storm events based on sedimentological archives. *Journal of African Earth Sciences*, 2020, 162, pp.103710. 10.1016/j.jafrearsci.2019.103710 . hal-02422247

HAL Id: hal-02422247

<https://hal.science/hal-02422247>

Submitted on 9 Jul 2020

HAL is a multi-disciplinary open access archive for the deposit and dissemination of scientific research documents, whether they are published or not. The documents may come from teaching and research institutions in France or abroad, or from public or private research centers.

L'archive ouverte pluridisciplinaire **HAL**, est destinée au dépôt et à la diffusion de documents scientifiques de niveau recherche, publiés ou non, émanant des établissements d'enseignement et de recherche français ou étrangers, des laboratoires publics ou privés.

Temporal approaches of historical extreme storm events based on sedimentological archives

Pierre Pouzet^{1,2*} and Mohamed Maanan²

¹ Université de Nantes, OSUNA – UMS 3281, Nantes, France.

² Université de Nantes, LETG – UMR CNRS 6554, Nantes, France.

* Corresponding author. E-mail: pierre.pouzet@univ-nantes.fr

Abstract

This paper presents the benefits of multiplying environmental indicators to better understand the impacts of past storm events on the environment. It aims to describe the methodological approaches used to reconstruct past extreme events from washover deposits, at the three main temporal scales used in scientific bibliography: i) the long timescale (Holocene, since 12 000 years BP), ii) the meso timescale (for the last millenary) and iii) the short timescale (Anthropocene, for the last centuries). This methodology is based on a “multiproxy” analysis using sedimentology, geochemistry and various methods of isotope dating. Linking these methods with other disciplines such as history, archaeology and meteorology leads us to confirm with great certainty the existence of these extreme events, and to expose their impacts on the environment and on past coastal societies. These different approaches enable us to enhance and refine our knowledge of coastal hazards, but also to apprehend possible storm influences in the context of climate change.

Keywords

Storm event, climate change, sedimentology, historical archives, washover deposit

Highlights

- Washover detections use various techniques depending on the timescale used.
- Three examples at the long, meso and short timescale are presented.
- Historical data are necessary to attest the stormy origin of a marine deposit.

29 **1. Introduction: from the coastal flooding to the washover deposit**

30 Marine flooding is nowadays densely studied as its damages are expected to increase in the
31 future (Hinkel et al., 2014). The flooding risk of coastal areas may significantly be enhanced
32 by the meaningful sea level rise expected by the IPCC (Pachauri et al., 2014), crossed with the
33 evolution of meteorological hazards activity (e.g. Paciorek et al., 2002; Page et al., 2010;
34 Ulbrich and Christoph, 1999) and the expected increase of worldwide coastal population
35 (Lutz and Samir, 2010; Neumann et al., 2015). Marine flooding is induced by intense
36 meteorological and oceanological parameters producing a significant morphogenic activity
37 over coastal environments (Figure 1). A “*storm surge*” is produced when the air pressure falls
38 down and the wind is significant (Doodson, 1924; Doodson and Warburg, 1942; Pugh, 1996),
39 but also when the wave set-up and swash, producing the run-up altogether, are powerful
40 (Cariolet, 2011a, 2011b; Stockdon et al., 2006). A significant storm surge can involve
41 allochthonous deposits, called “*washovers*”, that come from the marine domain and go to a
42 coastal depositional environment. Three different main mechanisms can produce
43 “*washovers*” deposits from an “*overwash*” process (Donnelly et al., 2004) :

44 i) The “*overflowing*” stays the rarest case because it requires an exceptional water level. The
45 level has to be higher than the protecting barrier or dike (Figure 1). It is probably one of the
46 most dangerous processes because after the retreat of the tide, the water remains blocked by
47 the dike in the coastal low areas (Shimozono and Sato, 2016). ii) The “*overtopping*” by the
48 action of the waves corresponds to the crossing of waves over dunes or dikes. They propel
49 water over the structure or dune (Figure 1). The water level is not higher than the height of the
50 protecting barrier. The significance of the crossing is mainly determined by the amplitude of
51 the wave swash, but also by the direction and force of the wind influencing water projections
52 (Leroy et al., 2015). iii) The breach of a protecting barrier (dune or dike) is the last marine
53 submersion mechanism (Figure 1). It can be induced by the first two mechanisms presented
54 above, and it is the one that can have the most human damages in coastal areas. It may be
55 punctual, in sections or sometimes characterized by a complete rupture. Even if protective
56 infrastructure serves to protect from the issues of the marine flooding hazards, peoples
57 remains directly exposed during destruction (even partial) of these barriers (Kolen et al.,
58 2002). Breaches also induce a coarser marine deposit than overtopping and overflowing
59 processes, with a grain size distribution from thicker to thinner sediment until the closing of
60 the lagoon. Their standard sedimentological signature is exposed in Figure 2.

61 To characterize an extreme event by sedimentology and to detect these washovers, three
62 questions arise: i) *How to identify a marine layer and differentiate it from traditional lagoon,*
63 *marsh or lake facies?* Thanks to sedimentological analyses, many indicators such as particle
64 size and geochemistry are used to characterize the origin of sediments (Maanan et al., 2015).
65 Marine deposits are then identified and underlined as allochthonous of the marsh (Pouzet et
66 al., 2019). ii) *When was the identified marine layer deposited in this coastal depositional*

67 *environment?* After detecting the marine layers through sedimentological analyses, the
68 sedimentary core is then dated to estimate their dates of deposit periods. This isotopic dating
69 is done either by sediments from surface facies (e.g. Abrantes et al., 2008; Cuellar-Martinez et
70 al., 2017), or by the organic elements present in the core (e.g. Bregy et al., 2018; Feal-Pérez et
71 al., 2014). These methods can be used to estimate the precise age or period when the marine
72 layers settled. iii) *How can we ensure that the marine layer comes from a natural hazard?*
73 Once the marine layer has been dated, historical data can be used to accurately characterize
74 the hazards that have induced the “*overwash*” process (Athimon and Maanan, 2018; Garnier
75 et al., 2018; Liu et al., 2001). Direct estimation of return periods can lead to many reserves,
76 especially on macrotidal coasts. Linking this method with a statistical study can, however,
77 offer much stronger conclusions. As with the work of Mann et al. (2009), it can allow an
78 estimation of recurrence intervals on a broader scale. Data on relative sea level and climatic
79 variations are essential to build an accurate estimation of the return periods of extreme events
80 (Goslin et al., 2018).

81 This paper presents three different methodologies used to detect past storm or phases of high
82 storminess at three different timescales (Pouzet, 2018) : the long term (at the Holocene scale),
83 the mesoscale (corresponding to the last millennia), and the short term (the last centuries or
84 decades). At these three timescales, a combination of methods is proposed to answer these
85 three different questions, allowing the link between a marine deposit and a past storm or a
86 phase of high storminess activity. Three distinct methodologies are detailed, including the
87 choice of a relevant coastal depositional environment, of the fieldwork techniques according
88 to the sediment type, the laboratories analyses and the potential discussion that can be set at
89 the three timescales determined. Benefits and limits of each methodology are also exposed.
90 They give a complete display of these three accurate combinations of methods discussed in
91 this paper that scientist may use to detect past extreme storm event from sedimentological
92 archives.

93 **2. State of art of methodological approaches to detect past storm deposits**

94 The first reconstructions of ancient tropical cyclones from the Gulf of Mexico, in a coastal
95 lagoon in Alabama, were published by Liu and Fearn (1993). The sedimentological method
96 was then synthesized in a second study in Florida (Liu and Fearn, 2000). It became widely
97 recognized scientifically from the early 2000s, and was then largely expanded throughout the
98 world. The method is based on the analysis of coastal marine sediment deposition transported
99 by extreme events and deposited in a marsh, lagoon or coastal lake. Liu and Fearn (2000,
100 1993) also discuss a relationship between the intensity of the past extreme event and its
101 sedimentological signature. They suggest a direct relationship between the deposition
102 structure and the intensity of the hazard. This link is still being discussed nowadays, as the
103 size and extent of these deposits also appear to depend as much on hazard-related

104 meteorological parameters as on the geomorphological characteristics of the cored
105 environment (Morton, 2002; Otvos, 2002; Sallenger, 2000).

106 As mentioned in many recent reviews (Clarke and Rendell, 2009; Kaniewski et al., 2016;
107 Oliva et al., 2017; Xiong et al., 2018), this method has grown considerably since the 2000s,
108 and is still widely used worldwide today. The United States, along the North American coasts
109 and the Caribbean Sea (e.g. Donnelly et al., 2001; J. P. Donnelly et al., 2004; Donnelly and
110 Woodruff, 2007; Lambert et al., 2008; Noren et al., 2002; Parris et al., 2009; Scileppi and
111 Donnelly, 2007; Scott et al., 2003) was the first place where this characteristic method
112 significantly developed in the early 21st century. It was then expanded worldwide with some
113 notable examples of works in Oceania (Hayne and Chappell, 2001; May et al., 2016, 2015;
114 Nott et al., 2009; Nott and Hayne, 2001) ; Asia (Liu et al., 2001; Williams et al., 2015;
115 Woodruff et al., 2009; Yu et al., 2009) ; Africa (Bozzano et al., 2002; Khalfaoui et al., 2019) ;
116 in the North Sea (Chang et al., 2006; Jong et al., 2006) ; or in South America (Oliveira et al.,
117 2014; Ramírez-Herrera et al., 2012). In western Europe, several studies have analyzed “*cliff*
118 *top storm deposits*” (e.g. Fichaut and Suanez, 2011; Hall et al., 2006; Hansom et al., 2008;
119 Hansom and Hall, 2009; Suanez et al., 2009; Williams and Hall, 2004), Mediterranean
120 lagoonal sequences (e.g. Abad et al., 2019; Degeai et al., 2015; Kaniewski et al., 2016;
121 Sabatier et al., 2012, 2010) and only few works have been conducted on the French Atlantic
122 coast (Baltzer et al., 2014; Poirier et al., 2017; Sorrel et al., 2009; Van Vliet Lanoe et al.,
123 2014). The British Isles (e.g. Devoy et al., 1996; Kylander et al., 2019; Oldfield et al., 2010;
124 Orme et al., 2015; Wilson et al., 2004), Scandinavia (e.g. Björckl and Clemmensen, 2004;
125 Bondevik et al., 2019; Jong et al., 2006), and Portugal (e.g. Andrade et al., 2004; Dawson et
126 al., 1995; Hindson and Andrade, 1999) have also been deeply studied, mainly from
127 sedimentological deposits.

128 The first indicators of marine deposition mainly focused on changes in grain sizes. First works
129 compared sandy marine deposits and lagoon continental clays/silts (Liu and Fearn, 1993). The
130 range of indicators available has then grown rapidly over the years and published works
131 (Clarke and Rendell, 2009; Kaniewski et al., 2016; Xiong et al., 2018). Organic matter (OM),
132 geochemistry, radiography, pollen, foraminifera, colorimetry, magnetic susceptibility, clay
133 minerals or several fauna assemblages are commonly used as evidence of a brutal
134 environmental change in the stratigraphy of a coastal marsh.

135 This method was also extended from the early 2000s to the analysis of tsunami deposits, as
136 mentioned in the works conducted along the Portuguese coasts. The study of tsunami deposits
137 was used there to detect the event of 1755 (e.g. Costa et al., 2012; Cunha et al., 2010; Oliveira
138 et al., 2009). New Zealand’s coasts are also the subject of numerous studies of tsunami
139 deposits from the 2000s onwards (e.g. Chagué-Goff et al., 2002; Goff et al., 2004, 2001). The
140 method then extends across the entire Pacific Ocean coastline (e.g. Goto et al., 2012, 2010,
141 2007; May et al., 2016; Nanayama et al., 2000; Pinegina and Bourgeois, 2001; Ramirez-

142 Herrera et al., 2007; Scheffers and Kelletat, 2003). As a result of this extensive work, the
143 geochemistry indicator has been popularized as a reliable indicator in sedimentological
144 research tracing the extreme coastal paleoevents in the world (Chagué-Goff et al., 2017). This
145 indicator is now also widely used in sedimentological studies of past cyclones (e.g. Das et al.,
146 2013; Oliva et al., 2017; Xiong et al., 2018). Distinction between stormy and tsunami deposits
147 is a problem still strongly debated today as these two marine deposits stay similar (Davies and
148 Haslett, 2000; Lario et al., 2010; Xiong et al., 2018). A presentation of the three timescales
149 employed is exposed in the Figure 3.

150 **3. Methodology adapted to different temporal approaches**

151 **3.1. Selection of the study sites**

152 The methodology used, detailed into Figure 4, is varied and combines different data collection
153 and analysis techniques. The first step is to select the sampling area. The study areas are
154 chosen according to three criteria: i) they must correspond to lowland coastal areas, as back
155 barrier environment; ii) they mustn't have been impacted by mankind iii) and these areas have
156 to be located in spaces with tempestuous activities dating back to several centuries, according
157 to local studies.

158 We first selected several study sites using a century-long diachronic study from Geographic
159 Information Systems (GIS). We were able to retrieve the Cassini's maps from the end of the
160 XVIIIth century, from the Etat-Major map (XIXth century) and the first aerial photographs
161 taken around 1950. These different data were imported, georeferenced and processed in a GIS
162 according to the method extracted from Pouzet et al. (2015). These data allow us to better
163 understand the recent evolution of the selected sites and to estimate the origin of potential
164 human impacts. The second selection concerns the analysis of topo-bathymetric data. It
165 allows us to analyse the topography and the precise bathymetry, in order to evaluate the
166 current geomorphology of the selected sites. They especially enable us to obtain precisely the
167 altitude of the protective sandy barriers and the protected lowlands cored. We were able to
168 produce a few geomorphological sections to choose the most relevant sites to study extreme
169 events deposits. Finally, we have affined our selection on lands that are regularly impacted by
170 storms (Athimon and Maanan, 2018; Feuillet et al., 2012; Le Roy et al., 2015). After selecting
171 the study areas, sampling stations have to be selected. Coring too close to the protecting
172 barrier can induce a smaller recording of marine deposits. During the deposition process, the
173 sandy barrier usually protects the lowlands located a few meters back according to Liu and
174 Fearn (2000). As the sandy barrier is thicker nowadays than in the past, its protecting action is
175 more important today than before. To detect millenary storms in lowland protected by a
176 barrier which have been thickened, a coring close to the actual barrier may offer the detection
177 of historical storms (Pouzet, 2018).

178 Two different coastal environments can be studied: i) back barriers lowlands areas and ii)
179 ancient coastal marshes that are sealed today, as peat bog of coastal lakes. Back barriers
180 coastal marshes records past storms that hit the region during the last decades or centuries,
181 depending of their age and the sedimentation rate assessed (e.g. Donnelly et al., 2004; Kenney
182 et al., 2016; May et al., 2015). This first type of coastal environment can be used to study past
183 storms at a short or meso timescale. In sealed ancient coastal marshes, sedimentation rates are
184 lower and can testify of an ancient lowland connected with the sea. They are used to assess
185 Holocene storms or phases of high storm activity and can be used in the long term timescale
186 analyses (e.g. Jong et al., 2006; Liu and Fearn, 1993; Orme et al., 2015; Stewart et al., 2017).

187 **3.2. Sampling methods**

188 Sedimentological cores allow us to study the vertical evolution of the sedimentary facies and
189 to analyse paleoenvironmental dynamics. They can include impacts of land use change (e.g.
190 Cuellar-Martinez et al., 2017; Maanan et al., 2014, 2018, 2015; Ning et al., 2018; Yim et al.,
191 2018), environmental changes such as sea level rise (e.g. Baltzer et al., 2015; Culver et al.,
192 2015; Fruergaard et al., 2015; Lambeck and Bard, 2000) and past storms detection (e.g.
193 Bennington and Farmer, 2014; Parris et al., 2010; Parsons, 1998).

194 Two coring methods are used depending on the type of environment and the time scale
195 considered: i) The « *Beeker* » handled corer is used into wet foreshore sediments (e.g.
196 Anderson et al., 1997; Fisher et al., 1992; Giuliani et al., 2015; Glew and Smol, 2016; Kanbar
197 et al., 2017). It can be used for the short term storm analysis of back barrier marshes with high
198 sedimentological dynamics (Figure 4). ii) The « *vibracore* » corer is used in sealed sediments
199 and can reach more important depths due to the compact sediment (e.g. DeVries-Zimmerman
200 et al., 2014; Francus et al., 2008; McGlue et al., 2015; Thompson and Baedke, 1995; Vance et
201 al., 1992; Yuan et al., 2013). It can be used into back barrier environments which are less
202 dynamics and wetter (natural salt marshes or “*schorres*”) into the mesoscale methodology. It
203 can also be used in ancient peat bog or sealed marshes for the long term analysis and the
204 detection of Holocene storms or phases of storminess increases (Figure 4).

205 Cores are then longitudinally opened in the laboratory. The first half is analyzed and the
206 second is archived and stored at 4°C to slow down deposit oxidation. A precise photograph is
207 taken as soon as the cores are opened to preserve the colors of the different facies. A
208 stratigraphic log is then constructed to describe the core (Figure 4). Sediments are
209 characterized by a visual litho-microstratigraphic analysis, to identify major changes in
210 granulometry, color, organic matter and to identify each macrofossil observed.

211 **3.3. Sedimentological analyses for past storm detection**

212 A high-resolution sampling is conducted before sedimentological analyses: a half centimeter
213 sampling is made for the geochemical signature determination and a centimeter sampling for
214 others treatments. Samples from each core will be analyzed by several scientific devices
215 (Figure 4). These analyses permit to characterize the physio-chemical and biological
216 parameters of sediments and to identify their origin (marine, continental or coastal). The
217 dating of the various sedimentary levels of cores is done using ^{210}Pb and ^{137}Cs for the last
218 century (e.g. Abrantes et al., 2008; Keen et al., 2004), and radiocarbon (^{14}C) for longer time
219 scales (e.g. Liu and Fearn, 2000b; Parris et al., 2010; Sorrel et al., 2009).

220 X-ray radiography by Scopix is used to provide images of the sedimentary structure of the
221 cores, the bioturbation, density and heterogeneity of the sediments, as well as the general
222 organization of the facies collected. This can also help identify fine sedimentological
223 variations which would be otherwise difficult to pinpoint, or even fine elements located in the
224 center of the core (shells, pebbles, remains of plants, etc.) when analyzing lithostratigraphy
225 (e.g. Coor et al., 2009; Migeon et al., 1998; Scott et al., 2003). Statistical analyses can be used
226 to select relevant indicators to characterize marine deposits made by storms (Pouzet et al.,
227 2019). Marine flooding is identified by a typical sedimentary sequence that alternates between
228 a level of marine sand (the washover fan) and the lagoon layers surrounding composed of
229 vases or silts with continental chemical influence. The marine sand can also be identified by
230 its biology with a significant presence of marine species.

231 3.3.1. The long scale analysis of Holocene periods of high storm activity

232 After extracting a core from a sealed coastal marsh with a “vibracore” corer, samples with
233 high carbon concentration or shell or plants remains are dated with the ^{14}C isotope (Figure 4).
234 The samples are burned at 500°C in a 1 L muffle furnace for four hours, in order to assess the
235 organic matter content by the loss in the ignition process (Santisteban et al., 2004). OM
236 proportion allows us to understand the paleoenvironmental changes of the study site, an
237 important parameter in the long scale analysis. Grain size is measured with a Malvern
238 Mastersizer 2000 © particle size analyzer, after a 5% sodium hexametaphosphate dispersion
239 (Gee and Or, 2002). Sand, silt and clays proportion can be extracted according to the Blott
240 and Pye (2001) classification, and a sand dominated content generally testify of the marine
241 origin of the sediment. Sedimentological high-resolution elemental analyses are evaluated
242 using an Avaatech© X-ray fluorescence (XRF) core scanner. Element intensities are
243 normalized by the total intensity (Bouchard et al., 2011; Martin et al., 2014). Strontium (Sr)
244 and Calcium (Ca) are the two elements which are mostly cited as marine (e.g. Chagué-Goff et
245 al., 2017; Pouzet et al., 2019; Roy et al., 2010). Other possibilities of marine proxy are also
246 mentioned in bibliography, including foraminifera (e.g. Alday et al., 2006; Hippensteel and
247 Martin, 1999), molluscan assemblages, (e.g. Bettinelli et al., 2018), pollens (e.g. Jong et al.,
248 2006), or clay mineral (e.g. Sabatier et al., 2010) analyses.

249 Marine layers are then extracted after identifying the sediment origins of each facies. To
250 prove that the marine layers have been deposited during a Holocene storm phase, a
251 comparison with other geological works from the scientific bibliography is required (Figure
252 3). At the Holocene scale, storm phases can be identified from several geological methods,
253 such as other similar back barrier analyses (e.g. Liu and Fearn, 1993; May et al., 2016;
254 Sabatier et al., 2012), “*cliff top storm deposits*” detection (e.g. Hall et al., 2006; Hansom and
255 Hall, 2009; Williams and Hall, 2004), bay sedimentation (e.g. Baltzer et al., 2014; Poirier et
256 al., 2017; Van Vliet Lanoe et al., 2014), dune evolution (e.g. Clarke and Rendell, 2006;
257 Clemmensen et al., 2009; Jelgersma et al., 1995), beach ridges morphology (e.g. Nott et al.,
258 2009; Scheffers et al., 2012; Thompson and Baedke, 1995), coral distribution (e.g. Gardner et
259 al., 2005; Hongo, 2018; Scoffin, 1993), and speleothems (e.g. Frappier et al., 2007; Zhu et al.,
260 2017), tree-ring (e.g. Cook and Kairiukstis, 2013; Lafon and Speer, 2002; Nicolussi et al.,
261 2005) or diatom (e.g. Nodine and Gaiser, 2015; Stager et al., 2017) production. The crossing
262 of sedimentological deposits with all these methods can be made to assess Holocene storm
263 activity in the same oceanic basin.

264 The detection of storm phases at a large timescale gives us clues about Holocene storm
265 activity, underlying periods of increasing and decreasing storminess over the last 12 000
266 years. These phases can be linked to climate change influenced mechanisms, such as
267 atmospheric circulation patterns (e.g. Goslin et al., 2018; Poirier et al., 2017; Stewart et al.,
268 2017), temperature evolution (e.g. Sabatier et al., 2012; Sorrel et al., 2009; Van Vliet Lanoe et
269 al., 2017) or ecstatic sea level variation (e.g. Baltzer et al., 2014; Spencer et al., 1998; Tisdall
270 et al., 2013). As these different drivers can also be reconstructed in long timescales, they can
271 show correlation with Holocene storm phases regionally detected in sedimentology. It may
272 increase our understanding of atmospheric or oceanic storm influences.

273 3.3.2. The mesoscale analysis of millenary extreme events

274 A “*vibracore*” corer can be used to extract a core from less dynamic back barrier
275 environments such as natural salt marshes or “*schorres*” (Figure 4). Radiocarbon content and
276 upper sediments are then sampled to be dated with ^{14}C , ^{210}Pb and ^{137}Cs . A crossing of the two
277 dating methods gives important dating precision to the entire core. To increase precision of
278 the OM estimation, a LECO © carbon analyzer estimates the CO_2 percentage after a 1400°C
279 dioxygen burning and a mineral decarbonizing with sulfuric acid solution (Andrews et al.,
280 2008; Michaelson G. J. et al., 2011). Grain size and elemental analyses are also measured
281 with a Malvern Mastersizer 2000 © particle size analyzer, and a Avaatech© X-ray
282 fluorescence (XRF) core scanner (Bouchard et al., 2011; Gee and Or, 2002; Martin et al.,
283 2014). Marine geochemical ratios, extracted from a statistical study, are used (Pouzet et al.,
284 2019). As a positive correlation between lightness and carbonate content has already been
285 demonstrated (Mix et al., 1995), lightness is estimated by colorimetric analyses with a

286 Minolta© Cm-2600d spectrometer. The magnetic susceptibility, which has been previously
287 used with success in other paleoenvironmental studies is measured with a MS2E-1©
288 Bartington-type (Bloemendal and deMenocal, 1989; Wassmer et al., 2010).

289 Once the marine layers are detected, they can be linked to extreme events or precise past
290 storms thanks to historical archives (Figure 3) if the region has a dense historical
291 documentation (Liu et al., 2001). Numerous types of documents, such as ancient maps,
292 narrative sources (chronicles, diaries or memories) and documents preserved in libraries and
293 in regional archives (books of accounts, records of repairs, surveys conducted after a disaster,
294 barometric observations, newspapers for instance) can be used (Athimon and Maanan, 2018;
295 Pouzet et al., 2019). They expose observational and descriptive data on past extreme weather
296 hazards such as the descriptions of the storm and the damage caused, as well as impacts on
297 societies and their reactions and adaptation (Garnier et al., 2018; Sarrazin, 2012; Sauzeau,
298 2014). Before being used to reconstruct the history of storms and sea flooding over a
299 relatively long period, documents have to be studied, analyzed and criticized (Athimon et al.,
300 2016). A precise date can be assessed from historical archives for storms that hit the region
301 several centuries ago and that have been detected in sedimentology.

302 Building a precise millennial storm chronology is a relevant tool to understand storm
303 dynamics. Numerous synoptic oceano-climatological patterns such as the North Atlantic
304 Oscillation (NAO) and the El Nino Southern Oscillation (ENSO) are mainly modelled into the
305 last centuries, or in the late Holocene (e.g. Baker et al., 2015; D'Arrigo and Jacoby, 1991;
306 Trouet et al., 2012). To understand the influence of these patterns in storm dynamics, a
307 precise late Holocene storm chronology is required (e.g. Orme et al., 2016; Poirier et al.,
308 2017; Sorrel et al., 2009). In the Atlantic basin, this mesoscale sedimentological and historical
309 coupling may also show storm activity variations between the three climatological main
310 phases: the Medieval Warm Period (WMP), the Little Ice Age (LIA) and the Anthropogenic
311 actual warming (e.g. Degeai et al., 2015; Orme et al., 2016; Van Vliet Lanoe et al., 2014).
312 Understanding these evolutions is necessary to assess future stormy variations in this context
313 of climate change.

314 3.3.3. The short scale analysis of recent storms

315 The wet foreshore of a back barrier environment is cored with a “Beeker” type corer, and the
316 top of the core is sampled to be dated with ^{210}Pb and ^{137}Cs (Figure 4). As any
317 paleoenvironmental evolution of the study site is assessed at this short timescale study, OM
318 content is not analyzed. Grain size, elemental analyses, lightness and magnetic susceptibility
319 are also measured with a Malvern Mastersizer 2000 © particle size analyzer, a Avaatech© X-
320 ray fluorescence (XRF) core scanner, a Minolta© Cm-2600d spectrometer and an MS2E-1©
321 Bartington-type (Bouchard et al., 2011; Gee and Or, 2002; Mix et al., 1995; Wassmer et al.,

322 2010). New statistical grain size proxies, as deciles or quartiles, can be tested. Microtextural
323 characteristics of quartz grains can also be used as a proxy (e.g. P. Costa et al., 2012).

324 To be sure that the observed marine layers are related to a recent storm, numerous historical
325 data can be used (Figure 3). Local diaries offer interesting information about damages made
326 by past extreme events (Athimon and Maanan, 2018). National weather service's websites can
327 also present dense information about historical marine floodings (Pouzet et al., 2019). In
328 addition, sedimentological archives can also be linked to accurate meteorological data, such
329 as wind speed and direction, air pressure or precipitations (Pouzet et al., 2018b).
330 Meteorological reanalysis offers a dense dataset of meteorological parameters for the XIXth
331 and the XXth centuries (Weisse et al., 2009). As marine inputs testify about past marine
332 flooding in lowland areas, tide parameters can also be estimated in area undergoing a
333 significant tide gauge. It may assure that the past storm induced a temporally sea level rise,
334 and can precisely give the hour when the storm surge occurred during high tides (Kolen et al.,
335 2002). Finally, recent studies showing models of wave parameters during storm surges can
336 also offer additional information about the flooding which brought marine inputs in the
337 coastal marsh (Bertin et al., 2012).

338 Other biological correlations can be assessed to complement knowledge in recent storms. For
339 instance, Pouzet et al. (2018b) showed that a dendrochronological approach can complement
340 the sedimentological method to understand recent storm dynamics. Independently,
341 sedimentological and dendrochronological data exhibit the dating of some particularly
342 destructive storms in a specified area and their impacts on a back barrier coastal marsh and on
343 trees. The sedimentological study shows some of the strongest marine flooding reported, and
344 the tree-ring analysis offers an overview of the occurrence of the windiest storms at a forest
345 scale. This coupled approach requires the presence of a dune stand near the back barrier
346 environment cored.

347 **4. Three examples of storm detection from sedimentology at the three timescales**

348 **4.1. Long timescale series: The stormy period detection at the Yeu island**

349 Stormy phases can be detected in several sites of a same area. The study of Pouzet et al.
350 (2018a) has been conducted in Yeu island, a French island regularly impacted by storms
351 (Athimon and Maanan, 2018). Three old sealed coastal marshes, which are separated from the
352 sea by high dunes, have been cored (Figure 5). The lithostratigraphy of the first core extracted
353 in the Marais de la Guerche is mainly composed of peat. Its main peaty layer is interrupted by
354 a large 40 centimeter wide sandy sheet. A strong event has deeply impacted this lowland, with
355 a marine sandy layer observed from centimeter 10 to 51. The marine occurrence is confirmed
356 by the presence of *Bittium Reticulatum* marine shells, dated at 1800 cal y BP at centimeter 37,

357 and the high Ca and Sr values. The sharp contact between the lower peat and the marine layer
358 testifies of the suddenness of the event. It was produced by two consecutive increases in sand,
359 enhancing the mean grain size from 20 to 320 μm and decreasing the OM from 75 to 20% due
360 to the high increase of marine sands (from 15 to 80%) and the disappearance of OM-rich
361 peats. The onset of these two successive increases is estimated at 2070 and 1940 cal y BP.
362 The Marais de La Croix is the second coastal lowland cored. At the bottom of the core, the
363 environment is more energetic, with coarse sediments with low OM levels (10 to 20%), and
364 slight geochemical variations until cm. 55. An important event disturbs the environment near
365 2100 – 1950 cal y BP (50-55 cm). After this stormy period, there is a change in the
366 environment with a lower energetic depositional marsh with marked increases in OM (30 to
367 50%), notable mean grain size (20 to 10 μm), and Sr (0.7 to 0.5) decreases, until the top of the
368 core. The Coulee Verte is the last environment studied. Several storm incursions are reported
369 in the entire core, including a disturbance starting near centimeter 100, increasing the OM rate
370 from 40 to 60% from centimeter 100 to 90. This disturbance ends at centimeter 80, where a
371 significant grain size increase is estimated from 10 to 30 μm , and sandy (from 5 to 45 %) Ca
372 (8 to 10) and Sr (from 1.1 to 1.4) peaks are detected.

373 In Yeu Island, this significant storm phase which deeply disturbed the three cored marshes is
374 estimated around Anno Domini (Figure 5). It has been assessed around 2100-1950 cal y BP
375 thanks to the ^{14}C dating results of the three different cores. This storm series may have opened
376 a large breach in the Marais de la Guerche, which functioned as a permanent inlet for 1200
377 years (Pouzet et al., 2018a). From the crossing with other geological storm-related studies, we
378 can assess that the entire European coast underwent similar impacts near Anno Domini.
379 Degeai et al., 2015 observed a high Mediterranean stormy period in southern France between
380 2044 and 1993 cal y BP. A storm event was also reported in Brittany at 2060 cal y BP by Van
381 Vliet Lanoe et al. (2014). Peaks of storminess have been reported from 2090 to 1970 cal y BP
382 in western Wales (Orme et al., 2015). Lastly, the start of a transgressive dune building period
383 at 2200 cal y BP is due to strong wind activity with sand invasion in central western Portugal
384 (Clarke and Rendell, 2006). These bibliographic correlations prove the stormy origin of the
385 perturbation observed in the three Yeu island cores.

386 Overall, nine periods of storminess increases, called Yeu Stormy Periods (YSP), were
387 extracted from the three investigated cores analyzed in Pouzet et al., (2018a). YSP have then
388 been correlated with European paleo-environment studies from the scientific literature, in
389 order to extract five European Atlantic Stormy Events (EASE). EASE are global phases of
390 storm increase period at the scale of the European Atlantic coast, estimated around 600-300,
391 1700-1100, 2900-2500, 3500-3300, 5500-5100 and 7700-7100 cal y BP. From the correlation
392 with Holocene cold event estimated by Bond et al. (2001, 1997) from an ice rafted debris
393 study (and then extended worldwide by Wanner et al. (2011)), EASE are linked to the
394 Holocene cold climatic phases (Pouzet et al., 2018a). This hypothesis follows previous
395 correlations already established between European storm activity and cold Holocene phases,

396 which were particularly conducted by Degeai et al. (2015), Sabatier et al. (2010), and Vallve
397 and Martin-Vide (1998). Detection of Holocene storm phases from sedimentology can be a
398 useful tool to apprehend possible climatological influences of historical storm activity.

399 **4.2. Meso-timescale series: an historical extreme event detected in Brittany clarified by** 400 **ancient archives**

401 The Petite mer de Gâvres (PMG) is a French back barrier lagoon protected from the sea by a
402 high sandy dune in Brittany (Figure 6). The PMG paleoenvironment can be divided into two
403 different stages (Pouzet, 2018). The first one is at the base of the core (between cm. 115 and
404 280: pre- 768 \pm 230 AD; section A). It testifies about a calmer environment than the upper
405 centimeters of the core. A silty environment between cm. 180 and 280 is interrupted by
406 several sandy EE. It characterizes the end of the protecting dune construction, with significant
407 grain size and geochemical variations. The dune construction transits until a mudflat
408 environment isolated from the sea once the littoral spit formed, between cm. 115 and 180.
409 This environment is composed of dense clays, rich of continental elements. The second main
410 stage characterizing the construction of this environment corresponds to the upper part of the
411 core (cm. 0-115: post-768 \pm 230 AD period; section B). This section is more dynamic than
412 section A, with a dominance of marine sediments. *Salicornia* vegetation testifies about a salt
413 marsh environment undergoing tidal ranges. A succession of important extreme events
414 deposits contributed to the formation of an important marine sandy deposit behind the
415 protecting dune, including a 1445 \pm 40 AD impacting event recorded at centimeter 79. It has
416 been dated with the crossing of ^{14}C and $^{210}\text{Pb}/^{137}\text{Cs}$ methods. This extreme event induced a
417 significant mean grain size increase from 59 to 512 μm , a fall of CO_2 from 7 to 1% due to the
418 sandy input, and an increase of lightness from 44 to 68% depending on the brighter color of
419 sands compared to clays and silts. As a 3cm wide diameter pebble has been detected in this
420 layer, geochemical analyses and radiography have been interrupted. The pebble is the
421 testament of about a highly impacting extreme event, producing significant oceanic dynamics,
422 which have deeply perturbed this coastal environment.

423 According to Athimon (2019) data, this significant impact can be linked to the storm that hit
424 the French Atlantic coast during the 27th – 28th January 1469 (n.st) AD, during a high Spring
425 tide assessed on January 28th. This storm induced significant damages into dikes and salt
426 marshes of the Bouin town, a former island submerged during the night. After this event,
427 historical records testify about the probable loss of 1 500 tons of salt, inducing major
428 economic losses (Athimon and Maanan, 2018). Important breaches appeared, numerous
429 ridges or roads were destroyed and several fertile lands became sterile (Athimon et al., 2016).
430 The bell tower of Saint-Aubin fell down and numerous trees were uprooted near Angers
431 (Athimon, 2019). Into the Retz region, the seigneurial taxes had to be reduced due to the
432 important impact of the marine flooding (Athimon, 2019; Sarrazin, 2012, 2005). The

433 information extracted from historical archives offers important details about economical and
434 societal impacts of storm, to complement environmental impacts detected in the
435 sedimentological sequence.

436 **4.3. Short timescale series: a recent storm inducing marine flooding and tree ring** 437 **disproportions in the Traicts du Croisic**

438 The Traicts du Croisic (TDC) is a French back barrier depositional environment located in
439 Loire-Atlantique, western France (Figure 7). From the analysis of several core extracted from
440 this environment, Pouzet et al. (2019) have identified twelve recent storms producing marine
441 flooding. One of them has been detected in the center of the lagoon at cm. 9 of the core. Mean
442 grain size increased from 80 to 175 μm , with a very slight increase of the tenth decile.
443 Strontium/Iron (Sr/Fe) and Calcium/Titanium (Ca/Ti) respectively increased from 0.08 to
444 0.15 and from 9 to 22. After the event, lightness started to increase from 40 to 50% and the
445 magnetic susceptibility slightly decreased from 1 to 0. A significant impact is also visible in
446 the radiography. With ^{210}Pb and ^{237}Cs dating, this marine layer has been deposited around
447 1977 AD, with a few years of error margin.

448 According to the recent historical documents, the two events of 2th December 1976 AD and
449 11th January 1978 AD could have caused this marine deposit. However, the 1976 AD storm
450 crossed a very low Neap tide, while a Spring tide occurred during the 1978 AD event. The
451 second date of 11th January 1978 AD is therefore used for this hypothesis. With a dozen
452 reported deaths, this storm crossed a large part of France involving important damages
453 reported from Dunkirk to the Gironde estuary. Numerous shipwrecks and marine flooding are
454 mentioned in French sources (Le Marin 1595, Metmar 101), and English documents for
455 British damages such as Steers et al. (1979). This Britannic source explains that “*many*
456 *houses were swept away by the waves*” during the marine flooding that impacted England.
457 Significant windy damages are mentioned in these various sources, including uprooted trees
458 or devastated houses in several parts of the two countries. 130km/h winds are reported in
459 England, and no maximum wind is documented in France (Pouzet, 2018). Precise information
460 can be extracted from these recent data. They attest to the stormy origin of the deposit and to
461 offers further information about the meteorological and oceanological parameters recorded
462 during the storm.

463 With an Index of Storm Disturbance estimated at 15 % during the 1977 – 1978 AD winter,
464 Pouzet et al. (2018b) showed that this storm has also impacted the dune stand located a few
465 kilometers north of the TDC. Based on tree ring growth disproportions, significant winds have
466 induced the perturbation of 15% of the sampled living trees, attesting the power of the
467 meteorological parameters during this storm. As both the dendrochronological and
468 sedimentological methods underlined storm impacts during the 1977 – 1978 AD winter, it

469 confirms that this storm has induced significant winds coming from the south west and an
470 important marine flooding near the TDC area. These hypotheses have also been confirmed by
471 historical archives. The relation between sedimentological and dendrochronological archives
472 has yet to be developed with further precision nowadays.

473 **5. Discussion and conclusions**

474 The three methodologies expose three different accurate combinations to detect past storm
475 impacts from sedimentological archives. However, several choices can be discussed to
476 improve the reliability of these results. At the Holocene timescale, the ^{14}C dating of sealed
477 coastal marshes or peat bogs reaches higher uncertainties than the $^{210}\text{Pb} / ^{137}\text{Cs}$ method used at
478 the two other timescales. It remains, however, the most used and accurate dating method
479 found in bibliography for Holocene sedimentological stratigraphy (e.g. Engel et al., 2012;
480 May et al., 2016; Page et al., 2010). This higher uncertainty does not allow the detection of a
481 precise past storm impact estimated to a day or a month. The detection of “*storminess*
482 *increasing phases*” rather than “*precise storm impacts*” is preferred. For ancient
483 reconstruction like the Holocene chronology, the only way to be certain of a past storm phase
484 is the comparison with other storminess found in various environmental studies (Pouzet et al.,
485 2018a). Unlike the methodology presented for the two other timescales, historical archives
486 cannot prove old events at a Holocene timescale. Caution must therefore always be applied
487 when interpreting the paleostorm or paleotsunami marine deposits at this timescale.
488 Furthermore, if several studies (mainly under a macrotidal regime) suggest a change in the
489 frequency or intensity of storm events throughout time (e.g. Donnelly and Woodruff, 2007;
490 Parris et al., 2010), the sedimentological study conducted must take the tide regime into
491 account. For a macrotidal coast, it remains challenging to discuss storm frequency or intensity
492 variations since a storm has to be crossed with a Spring tide to impact the coastal area. The
493 marine deposits detected only prove that storms have more or less impacted the environment
494 studied at a precise time.

495 Even if the meso-timescale study reaches high dating precisions, the combination of ^{14}C with
496 $^{210}\text{Pb} / ^{137}\text{Cs}$ dating techniques can be discussed. If the two methods are accurate and give
497 precise results, the stratigraphical layers that are concerned in the core by the crossing
498 between the upper $^{210}\text{Pb} / ^{137}\text{Cs}$ and the lower ^{14}C dating undergo high dating uncertainties.
499 Sediment compaction over the time has been proved to interfere with isotope dating. The
500 accumulation rate found can be different depending on the different dating methods used on a
501 same core, increasing uncertainties (Brain et al., 2015; Davidson et al., 2004; Edwards, 2006).
502 To avoid confusion in the determination of precise past storm dates, the crossing of the two
503 dating techniques has to be conducted on a layer that is not concerned by marine inputs. The
504 meso-timescale methodology also sets out the primary interest of historical archives. In
505 addition to confirming ancient sedimentological hypotheses with a low uncertainty, it offers
506 valuable understanding keys for finely characterizing the damage caused by the past events

507 detected. The socio-economic impacts of several centuries old storms are fully described and
508 the comparison of several past events can assess the society resiliency evolution across the
509 history (Athimon and Maanan, 2018).

510 A high resolution of past storm impacts is conducted at the Anthropocene timescale.
511 Meteorological data and recent newspaper articles gives the precise meteorological and
512 oceanological parameters producing these recent storms. Even if geochemical ratios have
513 become a common use into storm and tsunami sedimentological chronologies (Chagué-Goff
514 et al., 2017), these proxies have to be used after a precise analysis of the sediment
515 composition. The geochemical signature depends on the environment studied, and the ratios
516 built can differ depending on the oceanic basin and the continental inputs. A statistical study
517 with a Principal Component Analysis (PCA) and a dendrogram showing the main origin of
518 each element can be conducted (Pouzet et al., 2019). The dendrochronological crossing with
519 sedimentological impacts of storm can still be improved nowadays. These two methods
520 cannot be strictly crossed because their impacts come from distinct parameters (wind activity
521 for the dendrochronology and oceano/meteorological parameters for the sedimentology). Both
522 approaches are however efficient in their own way and their combination helps our
523 understanding of storm impact distribution in a specific area (Pouzet et al., 2018b).

524 In conclusion, this paper exposes methodologies used at three different timescales to
525 document sedimentological evidence of recent or ancient past storms, and Holocene storm
526 phases. Various coring methods, dating techniques and sedimentological analyses are
527 employed, depending on the main objectives of the paleostorm study conducted. They have
528 been summarized in Figure 8, which illustrates the main points of all the methods exposed in
529 this paper. We underline the necessity of proving the stormy origin of each marine deposit
530 detected and dated in the different cores. To attest to their oceano-atmospherical origin,
531 historical data study is essential. It proves that marine layers must come from natural coastal
532 hazards. History can be used to date past event accurately, sometimes with a defined day or
533 time. Depending on the timescale used, it can be scientific bibliography, written sources or
534 modern meteorological data such as reanalysis. It provides important information on the
535 impacts identified, characterizing the general magnitude of past events, offering precise
536 complements on societal and economic damages recorded, and the society reaction evolution
537 across the history. Based on these historical data, the three methodologies presented expose
538 accurate combinations of multidisciplinary methods discussed in this paper, used to detect
539 past extreme storm events extracted from sedimentological archives.

540 **6. Acknowledgements**

541 The authors gratefully acknowledge Cassandra Carnet for English corrections. Analyses,
542 operating costs and field measurements were funded by the DREAL-Pays de Loire and the

543 OSUNA through the research program OR2C-AXE3 (History of coastal risk). We also thank
544 editor-in-chief Dr. Mohamed Abdelsalam and two anonymous reviewers for their useful
545 comments, which helped us to greatly improve this article.

546 7. References

- 547 Abad, M., Muñoz, A.F., González-Regalado, M.L., Ruiz, F., Rodríguez-Vidal, J., Cáceres, L.M.,
548 Carretero, M.I., Monge, G., Pozo, M., Prudencio, M.I., Dias, M.I., Marques, R., Izquierdo, T.,
549 Tosquella, J., Romero, V., 2019. Evolución paleoambiental de una turbera finiholocena en el
550 sector suroccidental del Parque Nacional de Doñana (S.O. España). *Estudios Geológicos* 75,
551 087. <https://doi.org/10.3989/egeol.43417.514>
- 552 Abrantes, F., Alt-Epping, U., Lebreiro, S., Voelker, A., Schneider, R., 2008. Sedimentological record of
553 tsunamis on shallow-shelf areas: The case of the 1969 AD and 1755 AD tsunamis on the
554 Portuguese Shelf off Lisbon. *Marine Geology* 249, 283–293.
555 <https://doi.org/10.1016/j.margeo.2007.12.004>
- 556 Alday, M., Cearreta, A., Cachão, M., Freitas, M.C., Andrade, C., Gama, C., 2006. Micropalaeontological
557 record of Holocene estuarine and marine stages in the Corgo do Porto rivulet (Mira River, SW
558 Portugal). *Estuarine, Coastal and Shelf Science* 66, 532–543.
559 <https://doi.org/10.1016/j.ecss.2005.10.010>
- 560 Anderson, W.T., Mullins, H.T., Ito, E., 1997. Stable isotope record from Seneca Lake, New York:
561 Evidence for a cold paleoclimate following the Younger Dryas. *Geology* 25, 135–138.
562 [https://doi.org/10.1130/0091-7613\(1997\)025<0135:SIRFSL>2.3.CO;2](https://doi.org/10.1130/0091-7613(1997)025<0135:SIRFSL>2.3.CO;2)
- 563 Andrade, C., Freitas, M.C., Moreno, J., Craveiro, S.C., 2004. Stratigraphical evidence of Late Holocene
564 barrier breaching and extreme storms in lagoonal sediments of Ria Formosa, Algarve,
565 Portugal. *Marine Geology, Storms and their significance in coastal morpho-sedimentary
566 dynamics* 210, 339–362. <https://doi.org/10.1016/j.margeo.2004.05.016>
- 567 Andrews, J.E., Samways, G., Shimmield, G.B., 2008. Historical storage budgets of organic carbon,
568 nutrient and contaminant elements in saltmarsh sediments: Biogeochemical context for
569 managed realignment, Humber Estuary, UK. *Science of The Total Environment* 405, 1–13.
570 <https://doi.org/10.1016/j.scitotenv.2008.07.044>
- 571 Athimon, E., 2019. “Vimers de mer” et sociétés dans les provinces de la facade atlantique du
572 royaume de France (XIVe-XVIIIe siècle) (phdthesis). Université de Nantes.
- 573 Athimon, E., Maanan, M., 2018. Vulnerability, resilience and adaptation of societies during major
574 extreme storms during the Little Ice Age. *Climate of the Past Discussions* 2018, 1–28.
575 <https://doi.org/10.5194/cp-2018-62>
- 576 Athimon, E., Maanan, M., Sauzeau, T., Sarrazin, J.-L., 2016. Vulnérabilité et adaptation des sociétés
577 littorales aux aléas météo-marins entre Guérande et l’île de Ré, France (XIVe - XVIIIe siècle).
578 *Vertigo - la revue électronique en sciences de l’environnement* 16.
579 <https://doi.org/10.4000/vertigo.17927>
- 580 Baker, A., Hellstrom, J.C., Kelly, B.F.J., Mariethoz, G., Trouet, V., 2015. A composite annual-resolution
581 stalagmite record of North Atlantic climate over the last three millennia. *Scientific Reports* 5.
582 <https://doi.org/10.1038/srep10307>
- 583 Baltzer, A., Cassen, S., Walter-Simonnet, A.-V., Clouet, H., Lorin, A., Tessier, B., 2015. Variations du
584 niveau marin Holocène en Baie de Quiberon (Bretagne sud) : marqueurs archéologiques et
585 sédimentologiques. *Quaternaire. Revue de l’Association française pour l’étude du
586 Quaternaire* 26, 105–115. <https://doi.org/10.4000/quaternaire.7201>
- 587 Baltzer, A., Walter-Simonnet, A.-V., Mokeddem, Z., Tessier, B., Goubert, E., Cassen, S., Diffo, A., 2014.
588 Climatically-driven impacts on sedimentation processes in the Bay of Quiberon (south
589 Brittany, France) over the last 10,000 years. *The Holocene* 24, 679–688.
590 <https://doi.org/10.1177/0959683614526933>

591 Bennington, J.B., Farmer, E.C., 2014. Recognizing Past Storm Events in Sediment Cores Based on
592 Comparison to Recent Overwash Sediments Deposited by Superstorm Sandy, in: Learning
593 from the Impacts of Superstorm Sandy. Academic Press, Cambridge, pp. 89–106.

594 Bertin, X., Bruneau, N., Breilh, J.-F., Fortunato, A.B., Karpytchev, M., 2012. Importance of wave age
595 and resonance in storm surges: The case Xynthia, Bay of Biscay. *Ocean Modelling* 42, 16–30.
596 <https://doi.org/10.1016/j.ocemod.2011.11.001>

597 Bettinelli, M., Dillenburg, S.R., Lopes, R.P., Caron, F., 2018. Pleistocene molluscan assemblage in the
598 southern Coastal Plain of Rio Grande do Sul, Brazil: Implications in the evolution of a Barrier-
599 Lagoon System. *Journal of South American Earth Sciences* 86, 200–215.
600 <https://doi.org/10.1016/j.jsames.2018.06.014>

601 Björckl, S., Clemmensen, L.B., 2004. Aeolian sediment in raised bog deposits, Halland, SW Sweden: a
602 new proxy record of Holocene winter storminess variation in southern Scandinavia? *The*
603 *Holocene* 14, 677–688. <https://doi.org/10.1191/0959683604hl746rp>

604 Bloemendal, J., deMenocal, P., 1989. Evidence for a change in the periodicity of tropical climate
605 cycles at 2.4 Myr from whole-core magnetic susceptibility measurements. *Nature* 342, 897–
606 900. <https://doi.org/10.1038/342897a0>

607 Blott, S.J., Pye, K., 2001. Gradstat : a grain size distribution and statistics package for the analysis of
608 unconsolidated sediments. *Earth Surface Processes and Landforms* 26, 1237–1248.
609 <https://doi.org/10.1002/esp.261>

610 Bond, G., Kromer, B., Beer, J., Muscheler, R., Evans, M.N., Showers, W., Hoffmann, S., Lotti-Bond, R.,
611 Hajdas, I., Bonani, G., 2001. Persistent Solar Influence on North Atlantic Climate During the
612 Holocene. *Science* 294, 2130–2136. <https://doi.org/10.1126/science.1065680>

613 Bond, G., Showers, W., Cheseby, M., Lotti, R., Almasi, P., deMenocal, P., Priore, P., Cullen, H., Hajdas,
614 I., Bonani, G., 1997. A Pervasive Millennial-Scale Cycle in North Atlantic Holocene and Glacial
615 Climates. *Science* 278, 1257–1266. <https://doi.org/10.1126/science.278.5341.1257>

616 Bondevik, S., Løvdøen, T.K., Tøssebro, C., Årskog, H., Hjelle, K.L., Mehl, I.K., 2019. Between winter
617 storm surges – Human occupation on a growing Mid-Holocene transgression maximum
618 (Tapes) beach ridge at Longva, Western Norway. *Quaternary Science Reviews* 215, 116–131.
619 <https://doi.org/10.1016/j.quascirev.2019.05.006>

620 Bouchard, F., Francus, P., Pienitz, R., Laurion, I., 2011. Sedimentology and geochemistry of
621 thermokarst ponds in discontinuous permafrost, subarctic Quebec, Canada. *Journal of*
622 *Geophysical Research: Biogeosciences* 116, 14. <https://doi.org/10.1029/2011JG001675>

623 Bozzano, G., Kuhlmann, H., Alonso, B., 2002. Storminess control over African dust input to the
624 Moroccan Atlantic margin (NW Africa) at the time of maxima boreal summer insolation: a
625 record of the last 220 kyr. *Palaeogeography, Palaeoclimatology, Palaeoecology* 183, 155–168.
626 [https://doi.org/10.1016/S0031-0182\(01\)00466-7](https://doi.org/10.1016/S0031-0182(01)00466-7)

627 Brain, M.J., Kemp, A.C., Horton, B.P., Culver, S.J., Parnell, A.C., Cahill, N., 2015. Quantifying the
628 Contribution of Sediment Compaction to late Holocene Salt-Marsh Sea-Level
629 Reconstructions, North Carolina, USA. *Quaternary Research* 83, 41–51.
630 <https://doi.org/10.1016/j.yqres.2014.08.003>

631 Bregy, J.C., Wallace, D.J., Minzoni, R.T., Cruz, V.J., 2018. 2500-year paleotempestological record of
632 intense storms for the northern Gulf of Mexico, United States. *Marine Geology, Geological*
633 *Records of Extreme Wave Events* 396, 26–42. <https://doi.org/10.1016/j.margeo.2017.09.009>

634 Cariolet, J.-M., 2011a. Inondation des côtes basses et risques associés en Bretagne : vers une
635 redéfinition des processus hydrodynamiques liés aux conditions météo-océaniques et des
636 paramètres morfo-sédimentaires (phdthesis). Université de Bretagne occidentale - Brest.

637 Cariolet, J.-M., 2011b. Quantification du runup sur une plage macrotidale à partir des conditions
638 morphologiques et hydrodynamiques. *Géomorphologie : relief, processus, environnement*
639 17, 95–109. <https://doi.org/10.4000/geomorphologie.9315>

640 Chagué-Goff, C., Dawson, S., Goff, J.R., Zachariasen, J., Berryman, K.R., Garnett, D.L., Waldron, H.M.,
641 Mildenhall, D.C., 2002. A tsunami (ca. 6300 years BP) and other Holocene environmental
642 changes, northern Hawke's Bay, New Zealand. *Sedimentary Geology, Coastal Environment*

643 Change During Sea-Level Highstands 150, 89–102. <https://doi.org/10.1016/S0037->
644 0738(01)00269-X

645 Chagué-Goff, C., Szczuciński, W., Shinozaki, T., 2017. Applications of geochemistry in tsunami
646 research: A review. *Earth-Science Reviews* 165, 203–244.
647 <https://doi.org/10.1016/j.earscirev.2016.12.003>

648 Chang, T.S., Flemming, B.W., Tilch, E., Bartholomä, A., Wöstmann, R., 2006. Late Holocene
649 stratigraphic evolution of a back-barrier tidal basin in the East Frisian Wadden Sea, southern
650 North Sea: transgressive deposition and its preservation potential. *Facies* 52, 329–340.
651 <https://doi.org/10.1007/s10347-006-0080-2>

652 Clarke, M.L., Rendell, H.M., 2009. The impact of North Atlantic storminess on western European
653 coasts: A review. *Quaternary International, Hurricanes and Typhoons: From the Field Records*
654 *to the Forecast* 195, 31–41. <https://doi.org/10.1016/j.quaint.2008.02.007>

655 Clarke, M.L., Rendell, H.M., 2006. Effects of storminess, sand supply and the North Atlantic
656 Oscillation on sand invasion and coastal dune accretion in western Portugal. *The Holocene*
657 16, 341–355. <https://doi.org/10.1191/0959683606hl932rp>

658 Clemmensen, L.B., Murray, A., Heinemeier, J., de Jong, R., 2009. The evolution of Holocene coastal
659 dunefields, Jutland, Denmark: A record of climate change over the past 5000 years.
660 *Geomorphology* 105, 303–313. <https://doi.org/10.1016/j.geomorph.2008.10.003>

661 Cook, E.R., Kairiukstis, L.A., 2013. *Methods of Dendrochronology: Applications in the Environmental*
662 *Sciences*. Springer Science & Business Media, Netherlands.

663 Coor, J.L., Donoghue, J., Wang, Y., Das, O., Kish, S., Elsner, J., Hu, X.B., Niedoroda, A.W., Ye, M., 2009.
664 Development of a Long-Term Storm History for the Northwest Florida Coast Using Multiple
665 Proxies. *AGU Fall Meeting Abstracts* 11.

666 Costa, P., Andrade, C., Dawson, A.G., Mahaney, W.C., Freitas, M.C., Paris, R., Taborde, R., 2012.
667 Microtextural characteristics of quartz grains transported and deposited by tsunamis and
668 storms. *Sedimentary Geology* 275–276, 55–69.
669 <https://doi.org/10.1016/j.sedgeo.2012.07.013>

670 Costa, P.J.M., Andrade, C., Freitas, M., Oliveira, M., Lopes, V., Dawson, A., Moreno, J., Fatela, F.,
671 Jouanneau, J.-M., 2012. A tsunami record in the sedimentary archive of the central Algarve
672 coast, Portugal: Characterizing sediment, reconstructing sources and inundation paths. *The*
673 *Holocene* 22, 899–914. <https://doi.org/10.1177/0959683611434227>

674 Cuellar-Martinez, T., Ruiz-Fernández, A.C., Sanchez-Cabeza, J.-A., Alonso-Rodríguez, R., 2017.
675 Sedimentary record of recent climate impacts on an insular coastal lagoon in the Gulf of
676 California. *Quaternary Science Reviews* 160, 138–149.
677 <https://doi.org/10.1016/j.quascirev.2017.01.002>

678 Culver, S.J., Leorri, E., Mallinson, D.J., Corbett, D.R., Shazili, N.A.M., 2015. Recent coastal evolution
679 and sea-level rise, Setiu Wetland, Peninsular Malaysia. *Palaeogeography, Palaeoclimatology,*
680 *Palaeoecology* 417, 406–421. <https://doi.org/10.1016/j.palaeo.2014.10.001>

681 Cunha, P.P., Buylaert, J.P., Murray, A.S., Andrade, C., Freitas, M.C., Fatela, F., Munhá, J.M., Martins,
682 A.A., Sugisaki, S., 2010. Optical dating of clastic deposits generated by an extreme marine
683 coastal flood: The 1755 tsunami deposits in the Algarve (Portugal). *Quaternary*
684 *Geochronology, 12th International Conference on Luminescence and Electron Spin*
685 *Resonance Dating (LED 2008)* 5, 329–335. <https://doi.org/10.1016/j.quageo.2009.09.004>

686 D'Arrigo, R.D., Jacoby, G.C., 1991. A 1000-year record of winter precipitation from northwestern New
687 Mexico, USA: a reconstruction from tree-rings and its relation to El Niño and the Southern
688 Oscillation. *The Holocene* 1, 95–101. <https://doi.org/10.1177/095968369100100201>

689 Das, O., Wang, Y., Donoghue, J., Xu, X., Coor, J., Elsner, J., Xu, Y., 2013. Reconstruction of paleostorms
690 and paleoenvironment using geochemical proxies archived in the sediments of two coastal
691 lakes in northwest Florida. *Quaternary Science Reviews* 68, 142–153.
692 <https://doi.org/10.1016/j.quascirev.2013.02.014>

693 Davidson, G.R., Carnley, M., Lange, T., Galicki, S.J., Douglas, A., 2004. Changes in Sediment
694 Accumulation Rate in An Oxbow Lake Following Late 19Th Century Clearing of Land for

695 Agricultural Use: A ^{210}Pb , ^{137}Cs , and ^{14}C Study in Mississippi, USA. *Radiocarbon* 46, 755–
696 764. <https://doi.org/10.1017/S0033822200035797>

697 Davies, P., Haslett, S.K., 2000. Identifying storm or tsunami events in coastal basin sediments. *Area*
698 32, 335–336. <https://doi.org/10.1111/j.1475-4762.2000.tb00146.x>

699 Dawson, A.G., Hindson, R., Andrade, C., Freitas, C., Parish, R., Bateman, M., 1995. Tsunami
700 sedimentation associated with the Lisbon earthquake of 1 November AD 1755: Boca do Rio,
701 Algarve, Portugal. *The Holocene* 5, 209–215. <https://doi.org/10.1177/095968369500500208>

702 Degeai, J.-P., Devillers, B., Dezileau, L., Oueslati, H., Bony, G., 2015. Major storm periods and climate
703 forcing in the Western Mediterranean during the Late Holocene. *Quaternary Science Reviews*
704 129, 37–56. <https://doi.org/10.1016/j.quascirev.2015.10.009>

705 Devoy, R.J.N., Delaney, C., Carter, R.W.G., Jennings, S.C., 1996. Coastal Stratigraphies as Indicators of
706 Environmental Changes upon European Atlantic Coasts in the Late Holocene. *Journal of*
707 *Coastal Research* 12, 564–588.

708 DeVries-Zimmerman, S., Fisher, T.G., Hansen, E.C., Dean, S., 2014. Sand in lakes and bogs in Allegan
709 County, Michigan, as a proxy for eolian sand transport. *Geological Society of America. Special*
710 *Papers* 508, 111–131.

711 Donnelly, J.P., Butler, J., Roll, S., Wengren, M., Webb, T., 2004. A backbarrier overwash record of
712 intense storms from Brigantine, New Jersey. *Marine Geology, Storms and their significance in*
713 *coastal morpho-sedimentary dynamics* 210, 107–121.
714 <https://doi.org/10.1016/j.margeo.2004.05.005>

715 Donnelly, J.P., Roll, S., Wengren, M., Butler, J., Lederer, R., Webb, T., 2001. Sedimentary evidence of
716 intense hurricane strikes from New Jersey. *Geology* 29, 615–618.
717 [https://doi.org/10.1130/0091-7613\(2001\)029<0615:SEOIHS>2.0.CO;2](https://doi.org/10.1130/0091-7613(2001)029<0615:SEOIHS>2.0.CO;2)

718 Donnelly, J.P., Woodruff, J.D., 2007. Intense hurricane activity over the past 5,000 years controlled by
719 El Niño and the West African monsoon. *Nature* 447, 465–468.
720 <https://doi.org/10.1038/nature05834>

721 Doodson, A.T., 1924. Meteorological Perturbations of Sea-Level and Tides. *Geophysical Journal*
722 *International* 1, 124–147. <https://doi.org/10.1111/j.1365-246X.1924.tb05363.x>

723 Doodson, A.T., Warburg, H.D., 1942. Admiralty Manual of Tides. H. M. Stationary Office, London.

724 Edwards, R.J., 2006. Mid-to late-Holocene relative sea-level change in southwest Britain and the
725 influence of sediment compaction. *The Holocene* 16, 575–587.
726 <https://doi.org/10.1191/0959683606hi941rp>

727 Engel, M., Brückner, H., Pint, A., Wellbrock, K., Ginau, A., Voss, P., Grottker, M., Klasen, N., Frenzel,
728 P., 2012. The early Holocene humid period in NW Saudi Arabia – Sediments, microfossils and
729 palaeo-hydrological modelling. *Quaternary International, Geoarchaeology of Egypt and the*
730 *Mediterranean: reconstructing Holocene landscapes and human occupation history* 266,
731 131–141. <https://doi.org/10.1016/j.quaint.2011.04.028>

732 Feal-Pérez, A., Blanco-Chao, R., Ferro-Vázquez, C., Martínez-Cortizas, A., Costa-Casais, M., 2014. Late-
733 Holocene storm imprint in a coastal sedimentary sequence (Northwest Iberian coast). *The*
734 *Holocene* 24, 477–488. <https://doi.org/10.1177/0959683613520257>

735 Feuillet, T., Chauveau, É., Pourinet, L., 2012. Xynthia est-elle exceptionnelle ? Réflexions sur
736 l'évolution et les temps de retour des tempêtes, des marées de tempête, et des risques de
737 surcotes associés sur la façade atlantique française. *Noréis* n° 222, 27–44.

738 Fichaut, B., Suanez, S.S., 2011. Quarrying, transport and deposition of cliff-top storm deposits during
739 extreme events: Banneg Island, Brittany. *Marine Geology* 283, 36–55.
740 <https://doi.org/10.1016/j.margeo.2010.11.003>

741 Fisher, M.M., Brenner, M., Reddy, K.R., 1992. A simple, inexpensive piston corer for collecting
742 undisturbed sediment/water interface profiles. *Journal of Paleolimnology* 7, 157–161.
743 <https://doi.org/10.1007/BF00196870>

744 Francus, P., Bradley, R.S., Lewis, T., Abbott, M., Retelle, M., Stoner, J.S., 2008. Limnological and
745 sedimentary processes at Sawtooth Lake, Canadian High Arctic, and their influence on varve

746 formation. *Journal of Paleolimnology* 40, 963–985. <https://doi.org/10.1007/s10933-008->
747 9210-x

748 Frappier, A.B., Sahagian, D., Carpenter, S.J., González, L.A., Frappier, B.R., 2007. Stalagmite stable
749 isotope record of recent tropical cyclone events. *Geology* 35, 111–114.
750 <https://doi.org/10.1130/G23145A.1>

751 Fruergaard, M., Andersen, T.J., Nielsen, L.H., Johannessen, P.N., Aagaard, T., Pejrup, M., 2015. High-
752 resolution reconstruction of a coastal barrier system: impact of Holocene sea-level change.
753 *Sedimentology* 62, 928–969. <https://doi.org/10.1111/sed.12167>

754 Gardner, T.A., Côté, I.M., Gill, J.A., Grant, A., Watkinson, A.R., 2005. Hurricanes and Caribbean Coral
755 Reefs: Impacts, Recovery Patterns, and Role in Long-Term Decline. *Ecology* 86, 174–184.
756 <https://doi.org/10.1890/04-0141>

757 Garnier, E., Ciavola, P., Spencer, T., Ferreira, O., Armaroli, C., Mclvor, A., 2018. Historical analysis of
758 storm events: Case studies in France, England, Portugal and Italy. *Coastal Engineering* 134,
759 10–23. <https://doi.org/10.1016/j.coastaleng.2017.06.014>

760 Gee, G.W., Or, D., 2002. 2.4 Particle-Size Analysis, in: Dane, J.H., Topp, C.G. (Eds.), *SSSA Book Series*.
761 *Soil Science Society of America, San Diego*, pp. 255–293.
762 <https://doi.org/10.2136/sssabookser5.4.c12>

763 Giuliani, S., Bellucci, L.G., Romano, S., Piazza, R., Turetta, C., Vecchiato, M., Nhon, D.H., Frignani, M.,
764 2015. Exploring the possibility to detect recent temporal changes in highly disturbed
765 sedimentary records through sampling repetitions and core comparisons of porosity and
766 sand content. *Environmental Monitoring and Assessment* 187, 480.
767 <https://doi.org/10.1007/s10661-015-4702-4>

768 Glew, J.R., Smol, J.P., 2016. A push corer developed for retrieving high-resolution sediment cores
769 from shallow waters. *Journal of Paleolimnology* 56, 67–71. <https://doi.org/10.1007/s10933->
770 015-9873-z

771 Goff, J., Chagué-Goff, C., Nichol, S., 2001. Palaeotsunami deposits: a New Zealand perspective.
772 *Sedimentary Geology* 143, 1–6. [https://doi.org/10.1016/S0037-0738\(01\)00121-X](https://doi.org/10.1016/S0037-0738(01)00121-X)

773 Goff, J., McFadgen, B.G., Chagué-Goff, C., 2004. Sedimentary differences between the 2002 Easter
774 storm and the 15th-century Okoropunga tsunami, southeastern North Island, New Zealand.
775 *Marine Geology* 204, 235–250. [https://doi.org/10.1016/S0025-3227\(03\)00352-9](https://doi.org/10.1016/S0025-3227(03)00352-9)

776 Goslin, J., Fruergaard, M., Sander, L., Gałka, M., Menviel, L., Monkenbusch, J., Thibault, N.,
777 Clemmensen, L.B., 2018. Holocene centennial to millennial shifts in North-Atlantic storminess
778 and ocean dynamics. *Scientific Reports* 8, 12778. <https://doi.org/10.1038/s41598-018->
779 29949-8

780 Goto, K., Chagué-Goff, C., Goff, J., Jaffe, B., 2012. The future of tsunami research following the 2011
781 Tohoku-oki event. *Sedimentary Geology, The 2011 Tohoku-oki tsunami* 282, 1–13.
782 <https://doi.org/10.1016/j.sedgeo.2012.08.003>

783 Goto, K., Chavanich, S.A., Imamura, F., Kunthasap, P., Matsui, T., Minoura, K., Sugawara, D.,
784 Yanagisawa, H., 2007. Distribution, origin and transport process of boulders deposited by the
785 2004 Indian Ocean tsunami at Pakarang Cape, Thailand. *Sedimentary Geology* 202, 821–837.
786 <https://doi.org/10.1016/j.sedgeo.2007.09.004>

787 Goto, K., Miyagi, K., Kawamata, H., Imamura, F., 2010. Discrimination of boulders deposited by
788 tsunamis and storm waves at Ishigaki Island, Japan. *Marine Geology* 269, 34–45.
789 <https://doi.org/10.1016/j.margeo.2009.12.004>

790 Hall, A.M., Hansom, J.D., Williams, D.M., Jarvis, J., 2006. Distribution, geomorphology and lithofacies
791 of cliff-top storm deposits: Examples from the high-energy coasts of Scotland and Ireland.
792 *Marine Geology* 232, 131–155. <https://doi.org/10.1016/j.margeo.2006.06.008>

793 Hansom, J.D., Barltrop, N.D.P., Hall, A.M., 2008. Modelling the processes of cliff-top erosion and
794 deposition under extreme storm waves. *Marine Geology* 253, 36–50.
795 <https://doi.org/10.1016/j.margeo.2008.02.015>

796 Hansom, J.D., Hall, A.M., 2009. Magnitude and frequency of extra-tropical North Atlantic cyclones: A
797 chronology from cliff-top storm deposits. *Quaternary International, Hurricanes and*

798 Typhoons: From the Field Records to the Forecast 195, 42–52.
799 <https://doi.org/10.1016/j.quaint.2007.11.010>

800 Hayne, M., Chappell, J., 2001. Cyclone frequency during the last 5000 years at Curacoa Island, north
801 Queensland, Australia. *Palaeogeography, Palaeoclimatology, Palaeoecology* 168, 207–219.
802 [https://doi.org/10.1016/S0031-0182\(00\)00217-0](https://doi.org/10.1016/S0031-0182(00)00217-0)

803 Hindson, R.A., Andrade, C., 1999. Sedimentation and hydrodynamic processes associated with the
804 tsunami generated by the 1755 Lisbon earthquake. *Quaternary International* 56, 27–38.
805 [https://doi.org/10.1016/S1040-6182\(98\)00014-7](https://doi.org/10.1016/S1040-6182(98)00014-7)

806 Hinkel, J., Lincke, D., Vafeidis, A.T., Perrette, M., Nicholls, R.J., Tol, R.S.J., Marzeion, B., Fettweis, X.,
807 Ionescu, C., Levermann, A., 2014. Coastal flood damage and adaptation costs under 21st
808 century sea-level rise. *PNAS* 111, 3292–3297. <https://doi.org/10.1073/pnas.1222469111>

809 Hippensteel, S.P., Martin, R.E., 1999. Foraminifera as an indicator of overwash deposits, Barrier
810 Island sediment supply, and Barrier Island evolution: Folly Island, South Carolina.
811 *Palaeogeography, Palaeoclimatology, Palaeoecology* 149, 115–125.
812 [https://doi.org/10.1016/S0031-0182\(98\)00196-5](https://doi.org/10.1016/S0031-0182(98)00196-5)

813 Hongo, C., 2018. The Hydrodynamic Impacts of Tropical Cyclones on Coral Reefs of Japan: Key Points
814 and Future Perspectives, in: *Coral Reef Studies of Japan, Coral Reefs of the World*. Springer,
815 Singapore, pp. 163–173. https://doi.org/10.1007/978-981-10-6473-9_11

816 Jelgersma, S., Stive, M.J.F., van der Valk, L., 1995. Holocene storm surge signatures in the coastal
817 dunes of the western Netherlands. *Marine Geology* 125, 95–110.
818 [https://doi.org/10.1016/0025-3227\(95\)00061-3](https://doi.org/10.1016/0025-3227(95)00061-3)

819 Jong, R. de, Björck, S., Björkman, L., Clemmensen, L.B., 2006. Storminess variation during the last
820 6500 years as reconstructed from an ombrotrophic peat bog in Halland, southwest Sweden.
821 *Journal of Quaternary Science* 21, 905–919. <https://doi.org/10.1002/jqs.1011>

822 Kanbar, H.J., Montargès-Pelletier, E., Losson, B., Bihannic, I., Gley, R., Bauer, A., Villiéras, F., Manceau,
823 L., Samrani, A.G.E., Kazpard, V., Mansuy-Huault, L., 2017. Iron mineralogy as a fingerprint of
824 former steelmaking activities in river sediments. *Science of the Total Environment* 599–600,
825 540–553. <https://doi.org/10.1016/j.scitotenv.2017.04.156>

826 Kaniewski, D., Marriner, N., Morhange, C., Faivre, S., Otto, T., Campo, E.V., 2016. Solar pacing of
827 storm surges, coastal flooding and agricultural losses in the Central Mediterranean. *Scientific*
828 *Reports* 6. <https://doi.org/10.1038/srep25197>

829 Keen, T.R., Bentley, S.J., Chad Vaughan, W., Blain, C.A., 2004. The generation and preservation of
830 multiple hurricane beds in the northern Gulf of Mexico. *Marine Geology, Storms and their*
831 *significance in coastal morpho-sedimentary dynamics* 210, 79–105.
832 <https://doi.org/10.1016/j.margeo.2004.05.022>

833 Kenney, W.F., Brenner, M., Arnold, T.E., Curtis, J.H., Schelske, C.L., 2016. Sediment cores from
834 shallow lakes preserve reliable, informative paleoenvironmental archives despite hurricane-
835 force winds. *Ecological Indicators* 60, 963–969.
836 <https://doi.org/10.1016/j.ecolind.2015.08.046>

837 Khalfaoui, O., Dezileau, L., Degeai, J.-P., Snoussi, M., 2019. Reconstruction of past marine submersion
838 events (storms and tsunamis) on the North Atlantic coast of Morocco. *Natural Hazards and*
839 *Earth System Sciences Discussions* 1–14. <https://doi.org/10.5194/nhess-2019-130>

840 Kolen, B., Slomp, R., Jonkman, S.N., 2002. The impacts of storm Xynthia February 27–28, 2010 in
841 France: lessons for flood risk management. *Journal of Flood Risk Management* 6, 261–278.
842 <https://doi.org/10.1111/jfr3.12011>

843 Kylander, M.E., Söderlindh, J., Schenk, F., Gyllencreutz, R., Rydberg, J., Bindler, R., Cortizas, A.M.,
844 Skelton, A., 2019. It's in your glass: a history of sea level and storminess from the Laphroaig
845 bog, Islay (southwestern Scotland). *Boreas*. <https://doi.org/10.1111/bor.12409>

846 Lafon, C.W., Speer, J.H., 2002. Using dendrochronology to identify major ice storm events in oak
847 forests of southwestern Virginia. *Climate Research* 20, 41–54.

848 Lambeck, K., Bard, E., 2000. Sea-level change along the French Mediterranean coast for the past
849 30 000 years. *Earth and Planetary Science Letters* 175, 203–222.
850 [https://doi.org/10.1016/S0012-821X\(99\)00289-7](https://doi.org/10.1016/S0012-821X(99)00289-7)

851 Lambert, W.J., Aharon, P., Rodriguez, A.B., 2008. Catastrophic hurricane history revealed by organic
852 geochemical proxies in coastal lake sediments: a case study of Lake Shelby, Alabama (USA).
853 *Journal of Paleolimnology* 39, 117–131. <https://doi.org/10.1007/s10933-007-9101-6>

854 Lario, J., Luque, L., Zazo, C., Goy, J.L., Spencer, C., Cabero, A., Bardají, T., Borja, F., Dabrio, C.J., Civis,
855 J., González-Delgado, J.Á., Borja, C., Alonso-Azcárate, J., 2010. Tsunami vs. storm surge
856 deposits: a review of the sedimentological and geomorphological records of extreme wave
857 events (EWE) during the Holocene in the Gulf of Cadiz, Spain. *Zeitschrift für Geomorphologie*
858 54, 301–316.

859 Le Roy, S., Pedreros, R., André, C., Paris, F., Lecacheux, S., Marche, F., Vinchon, C., 2015. Coastal
860 flooding of urban areas by overtopping: dynamic modelling application to the Johanna storm
861 (2008) in Gâvres (France). *Natural Hazards and Earth System Sciences* 15, 2497–2510.
862 <https://doi.org/10.5194/nhess-15-2497-2015>

863 Leroy, S., Pedreros, R., André, C., Paris, F., Lecacheux, S., Marche, F., Vinchon, C., 2015. Coastal
864 flooding of urban areas by overtopping: dynamic modelling application to the Johanna storm
865 (2008) in Gâvres (France). *Natural Hazards and Earth System Science* 15, 2497–2510.
866 <https://doi.org/10.5194/nhess-15-2497-2015>

867 Liu, K., Fearn, M.L., 2000a. Reconstruction of Prehistoric Landfall Frequencies of Catastrophic
868 Hurricanes in Northwestern Florida from Lake Sediment Records. *Quaternary Research* 54,
869 238–245. <https://doi.org/10.1006/qres.2000.2166>

870 Liu, K., Fearn, M.L., 2000b. Holocene history of catastrophic hurricane landfalls along the Gulf of
871 Mexico coast reconstructed from coastal lake and marsh sediments, in: Zhu, H., Kamran, K.
872 (Eds.), *Current Stresses and Potential Vulnerabilities: Implications of Global Change for the*
873 *Gulf Coast Region of the United States*. Franklin Press, Plymouth, pp. 38–47.

874 Liu, K., Fearn, M.L., 1993. Lake-sediment record of late Holocene hurricane activities from coastal
875 Alabama. *Geology* 21, 793–796. [https://doi.org/10.1130/0091-7613\(1993\)021<0793:LSROLH>2.3.CO;2](https://doi.org/10.1130/0091-7613(1993)021<0793:LSROLH>2.3.CO;2)

876

877 Liu, K., Shen, C., Louie, K., 2001. A 1,000-Year History of Typhoon Landfalls in Guangdong, Southern
878 China, Reconstructed from Chinese Historical Documentary Records. *Annals of the*
879 *Association of American Geographers* 91, 453–464. <https://doi.org/10.1111/0004-5608.00253>

880

881 Lutz, W., Samir, K., 2010. Dimensions of global population projections: what do we know about
882 future population trends and structures? *Philosophical Transactions of the Royal Society of*
883 *London B: Biological Sciences* 365, 2779–2791. <https://doi.org/10.1098/rstb.2010.0133>

884 Maanan, Mehdi, Maanan, Mohamed, Rueff, H., Adouk, N., Zourarah, B., Rhinane, H., 2018. Assess the
885 human and environmental vulnerability for coastal hazard by using a multi-criteria decision
886 analysis. *Human and Ecological Risk Assessment: An International Journal* 24, 1642–1658.
887 <https://doi.org/10.1080/10807039.2017.1421452>

888 Maanan, Mehdi, Ruiz-Fernández, A.-C., Maanan, Mohamed, Fattal, P., Zourarah, B., Sahabi, M., 2014.
889 A long-term record of land use change impacts on sediments in Oualidia lagoon, Morocco.
890 *International Journal of Sediment Research* 29, 1–10.

891 Maanan, Mohamed, Saddik, M., Maanan, Mehdi, Chaibi, M., Assobhei, O., Zourarah, B., 2015.
892 Environmental and ecological risk assessment of heavy metals in sediments of Nador lagoon,
893 Morocco. *Ecological Indicators* 48, 616–626. <https://doi.org/10.1016/j.ecolind.2014.09.034>

894 Mann, M.E., Woodruff, J.D., Donnelly, J.P., Zhang, Z., 2009. Atlantic hurricanes and climate over the
895 past 1,500 years. *Nature* 460, 880–883. <https://doi.org/10.1038/nature08219>

896 Martin, L., Mooney, S., Goff, J., 2014. Coastal wetlands reveal a non-synchronous island response to
897 sea-level change and a palaeostorm record from 5.5 kyr to present. *The Holocene* 24, 569–
898 580. <https://doi.org/10.1177/0959683614522306>

899 May, S.M., Brill, D., Engel, M., Scheffers, A., Pint, A., Opitz, S., Wennrich, V., Squire, P., Kelletat, D.,
900 Brückner, H., 2015. Traces of historical tropical cyclones and tsunamis in the Ashburton Delta
901 (north-west Australia). *Sedimentology* 62, 1546–1572. <https://doi.org/10.1111/sed.12192>
902 May, S.M., Falvard, S., Norpoth, M., Pint, A., Brill, D., Engel, M., Scheffers, A., Dierick, M., Paris, R.,
903 Squire, P., Brückner, H., 2016. A mid-Holocene candidate tsunami deposit from the NW Cape
904 (Western Australia). *Sedimentary Geology* 332, 40–50.
905 <https://doi.org/10.1016/j.sedgeo.2015.11.010>
906 McGlue, M.M., Silva, A., Assine, M.L., Stevaux, J.C., Pupim, F. do N., 2015. Paleolimnology in the
907 Pantanal: Using Lake Sediments to Track Quaternary Environmental Change in the World's
908 Largest Tropical Wetland, in: *Dynamics of the Pantanal Wetland in South America, The*
909 *Handbook of Environmental Chemistry*. Springer, Cham, pp. 51–81.
910 https://doi.org/10.1007/698_2015_350
911 Michaelson G. J., Ping C. L., Jorgenson M. T., 2011. Methane and carbon dioxide content in eroding
912 permafrost soils along the Beaufort Sea coast, Alaska. *Journal of Geophysical Research:*
913 *Biogeosciences* 116, 10. <https://doi.org/10.1029/2010JG001387>
914 Migeon, S., Weber, O., Faugeres, J.-C., Saint-Paul, J., 1998. SCOPIX: A new X-ray imaging system for
915 core analysis. *Geo-Marine Letters* 18, 251–255. <https://doi.org/10.1007/s003670050076>
916 Mix, A.C., Harris, S.E., Janecek, T.R., 1995. Estimating lithology from nonintrusive reflectance spectra :
917 Leg 138. *Proceedings of the Ocean Drilling Program, Scientific Results* 138, 413–428.
918 Morton, R.A., 2002. Factors Controlling Storm Impacts on Coastal Barriers and Beaches: A Preliminary
919 Basis for near Real-Time Forecasting. *Journal of Coastal Research* 18, 486–501.
920 Nanayama, F., Shigeno, K., Satake, K., Shimokawa, K., Koitabashi, S., Miyasaka, S., Ishii, M., 2000.
921 Sedimentary differences between the 1993 Hokkaido-nansei-oki tsunami and the 1959
922 Miyakojima typhoon at Taisei, southwestern Hokkaido, northern Japan. *Sedimentary Geology*
923 135, 255–264. [https://doi.org/10.1016/S0037-0738\(00\)00076-2](https://doi.org/10.1016/S0037-0738(00)00076-2)
924 Neumann, B., Vafeidis, A.T., Zimmermann, J., Nicholls, R.J., 2015. Future Coastal Population Growth
925 and Exposure to Sea-Level Rise and Coastal Flooding - A Global Assessment. *PLOS ONE* 10, 34.
926 <https://doi.org/10.1371/journal.pone.0118571>
927 Nicolussi, K., Kaufmann, M., Patzelt, G., Der, J.P. van, Thurner, A., 2005. Holocene tree-line variability
928 in the Kauner Valley, Central Eastern Alps, indicated by dendrochronological analysis of living
929 trees and subfossil logs. *Vegetation History and Archaeobotany* 14, 221–234.
930 <https://doi.org/10.1007/s00334-005-0013-y>
931 Ning, W., Nielsen, A.B., Ivarsson, L.N., Jilbert, T., Åkesson, C.M., Slomp, C.P., Andrén, E., Broström, A.,
932 Filipsson, H.L., 2018. Anthropogenic and climatic impacts on a coastal environment in the
933 Baltic Sea over the last 1000 years. *Anthropocene* 21, 66–79.
934 <https://doi.org/10.1016/j.ancene.2018.02.003>
935 Nodine, E.R., Gaiser, E.E., 2015. Seasonal differences and response to a tropical storm reflected in
936 diatom assemblage changes in a southwest Florida watershed. *Ecological Indicators* 57, 139–
937 148. <https://doi.org/10.1016/j.ecolind.2015.04.035>
938 Noren, A.J., Bierman, P.R., Steig, E.J., Lini, A., Southon, J., 2002. Millennial-scale storminess variability
939 in the northeastern United States during the Holocene epoch. *Nature* 419, 821–824.
940 <https://doi.org/10.1038/nature01132>
941 Nott, J., Hayne, M., 2001. High frequency of 'super-cyclones' along the Great Barrier Reef over the
942 past 5,000 years. *Nature* 413, 508–512. <https://doi.org/10.1038/35097055>
943 Nott, J., Smithers, S., Walsh, K., Rhodes, E., 2009. Sand beach ridges record 6000 year history of
944 extreme tropical cyclone activity in northeastern Australia. *Quaternary Science Reviews* 28,
945 1511–1520. <https://doi.org/10.1016/j.quascirev.2009.02.014>
946 Oldfield, F., Battarbee, R.W., Boyle, J.F., Cameron, N.G., Davis, B., Evershed, R.P., McGovern, A.D.,
947 Jones, V., Thompson, R., Walker (née Wake), R., 2010. Terrestrial and aquatic ecosystem
948 responses to late Holocene climate change recorded in the sediments of Lochan Uaine,
949 Cairngorms, Scotland. *Quaternary Science Reviews* 29, 1040–1054.
950 <https://doi.org/10.1016/j.quascirev.2010.01.007>

- 951 Oliva, F., Peros, M., Viau, A., 2017. A review of the spatial distribution of and analytical techniques
952 used in paleotempestological studies in the western North Atlantic Basin: Progress in Physical
953 Geography: Earth and Environment 41, 171–190.
954 <https://doi.org/10.1177/0309133316683899>
- 955 Oliveira, F.M., Macario, K.D., Simonassi, J.C., Gomes, P.R.S., Anjos, R.M., Carvalho, C., Linares, R.,
956 Alves, E.Q., Castro, M.D., Souza, R.C.C.L., Marques Jr., A.N., 2014. Evidence of strong storm
957 events possibly related to the little Ice Age in sediments on the southern coast of Brazil.
958 Palaeogeography, Palaeoclimatology, Palaeoecology, Continental and Coastal Marine
959 Records of Centennial to Millennial Changes in South American Climate since the Last Glacial
960 Maximum 415, 233–239. <https://doi.org/10.1016/j.palaeo.2014.03.018>
- 961 Oliveira, M.A., Andrade, C., Freitas, M.C., Costa, P.J., 2009. Modeling Volume Transfer between
962 Beach-Foredune and the Backshore by the 1755 Lisbon Tsunami at Boca Do Rio Lowland,
963 Algarve (Portugal). Journal of Coastal Research 2, 1547–1551.
- 964 Orme, L.C., Davies, S.J., Duller, G. a. T., 2015. Reconstructed centennial variability of Late Holocene
965 storminess from Cors Fochno, Wales, UK. Journal of Quaternary Science 30, 478–488.
966 <https://doi.org/10.1002/jqs.2792>
- 967 Orme, L.C., Reinhardt, L., Jones, R.T., Charman, D.J., Barkwith, A., Ellis, M.A., 2016. Aeolian sediment
968 reconstructions from the Scottish Outer Hebrides: Late Holocene storminess and the role of
969 the North Atlantic Oscillation. Quaternary Science Reviews 132, 15–25.
970 <https://doi.org/10.1016/j.quascirev.2015.10.045>
- 971 Otvos, E.G., 2002. Discussion of “Prehistoric Landfall Frequencies of Catastrophic Hurricanes...” (Liu
972 and Fearn, 2000). Quaternary Research 57, 425–428.
973 <https://doi.org/10.1006/qres.2002.2333>
- 974 Pachauri, R.K., Allen, M.R., Barros, V.R., Broome, J., Cramer, W., Christ, R., Church, J.A., Clarke, L.,
975 Dahe, Q., Dasgupta, P., Dubash, N.K., Edenhofer, O., Elgizouli, I., Field, C.B., Forster, P.,
976 Friedlingstein, P., Fuglestad, J., Gomez-Echeverri, L., Hallegatte, S., Hegerl, G., Howden, M.,
977 Jiang, K., Jimenez Cisneros, B., Kattsov, V., Lee, H., Mach, K.J., Marotzke, J., Mastrandrea,
978 M.D., Meyer, L., Minx, J., Mulugetta, Y., O’Brien, K., Oppenheimer, M., Pereira, J.J., Pichs-
979 Madruga, R., Plattner, G.-K., Pörtner, H.-O., Power, S.B., Preston, B., Ravindranath, N.H.,
980 Reisinger, A., Riahi, K., Rusticucci, M., Scholes, R., Seyboth, K., Sokona, Y., Stavins, R., Stocker,
981 T.F., Tschakert, P., van Vuuren, D., van Ypserle, J.-P., 2014. Climate Change 2014: Synthesis
982 Report. Contribution of Working Groups I, II and III to the Fifth Assessment Report of the
983 Intergovernmental Panel on Climate Change. IPCC, Geneva, Switzerland.
- 984 Paciorek, C.J., Risbey, J.S., Ventura, V., Rosen, R.D., 2002. Multiple Indices of Northern Hemisphere
985 Cyclone Activity, Winters 1949–99. Journal of Climate 15, 1573–1590.
986 [https://doi.org/10.1175/1520-0442\(2002\)015<1573:MIONHC>2.0.CO;2](https://doi.org/10.1175/1520-0442(2002)015<1573:MIONHC>2.0.CO;2)
- 987 Page, M.J., Trustrum, N.A., Orpin, A.R., Carter, L., Gomez, B., Cochran, U.A., Mildenhall, D.C., Rogers,
988 K.M., Brackley, H.L., Palmer, A.S., Northcote, L., 2010. Storm frequency and magnitude in
989 response to Holocene climate variability, Lake Tutira, North-Eastern New Zealand. Marine
990 Geology, From mountain source to ocean sink – the passage of sediment across an active
991 margin, Waipaoa Sedimentary System, New Zealand 270, 30–44.
992 <https://doi.org/10.1016/j.margeo.2009.10.019>
- 993 Parris, A.S., Bierman, P.R., Noren, A.J., Prins, M.A., Lini, A., 2010. Holocene paleostorms identified by
994 particle size signatures in lake sediments from the northeastern United States. Journal of
995 Paleolimnology 43, 29–49. <https://doi.org/10.1007/s10933-009-9311-1>
- 996 Parris, A.S., Bierman, P.R., Noren, A.J., Prins, M.A., Lini, A., 2009. Holocene paleostorms identified by
997 particle size signatures in lake sediments from the northeastern United States. J Paleolimnol
998 43, 29–49. <https://doi.org/10.1007/s10933-009-9311-1>
- 999 Parsons, M.L., 1998. Salt Marsh Sedimentary Record of the Landfall of Hurricane Andrew on the
1000 Louisiana Coast: Diatoms and Other Paleoindicators. Journal of Coastal Research 14, 939–
1001 950. <https://doi.org/10.2307/4298846>

1002 Pinegina, T.K., Bourgeois, J., 2001. Historical and paleo-tsunami deposits on Kamchatka, Russia: long-
1003 term chronologies and long-distance correlations. *Natural Hazards and Earth System Sciences*
1004 1, 177–185. <https://doi.org/10.5194/nhess-1-177-2001>

1005 Poirier, C., Tessier, B., Chaumillon, E., 2017. Climate control on late Holocene high-energy
1006 sedimentation along coasts of the northeastern Atlantic Ocean. *Palaeogeography,*
1007 *Palaeoclimatology, Palaeoecology* 485, 784–797.
1008 <https://doi.org/10.1016/j.palaeo.2017.07.037>

1009 Pouzet, P., 2018. Étude des paléoévénements extrêmes le long de la côte atlantique française :
1010 Approches sédimentologiques, dendrochronologiques et historiques (phdthesis). Université
1011 de Nantes. NNT : 2018NANT2035

1012 Pouzet, P., Creach, A., Godet, L., 2015. Dynamique de la démographie et du bâti dans l’ouest du
1013 Marais poitevin depuis 1705. *Norois* 234, 83–96. <https://doi.org/10.4000/norois.5589>

1014 Pouzet, P., Maanan, M., Piotrowska, N., Baltzer, A., Stéphan, P., Robin, M., 2018a. Chronology of
1015 Holocene storm events along the European Atlantic coast: New data from the Island of Yeu,
1016 France. *Progress in Physical Geography: Earth and Environment* 42, 431–450.
1017 <https://doi.org/10.1177/0309133318776500>

1018 Pouzet, P., Maanan, M., Schmidt, S., Athimon, E., Robin, M., 2019. Correlating three centuries of
1019 historical and geological data for the marine deposit reconstruction of two depositional
1020 environments of the French Atlantic coast. *Marine Geology* 407, 181–191.
1021 <https://doi.org/10.1016/j.margeo.2018.10.014>

1022 Pouzet, P., Robin, M., Decaulne, A., Gruchet, B., Maanan, M., 2018b. Sedimentological and
1023 dendrochronological indicators of coastal storm risk in western France. *Ecological Indicators*
1024 90, 401–415. <https://doi.org/10.1016/j.ecolind.2018.03.022>

1025 Pugh, D.T., 1996. Tides, surges and mean sea-level. John Wiley & Sons Ltd, New Jersey.

1026 Ramirez-Herrera, M.T., Cundy, A., Kostoglodov, V., Carranza-Edwards, A., Morales, E., Metcalfe, S.,
1027 2007. Sedimentary record of late-Holocene relative sea-level change and tectonic
1028 deformation from the Guerrero Seismic Gap, Mexican Pacific Coast. *The Holocene* 17, 1211–
1029 1220. <https://doi.org/10.1177/0959683607085127>

1030 Ramírez-Herrera, M.-T., Lagos, M., Hutchinson, I., Kostoglodov, V., Machain, M.L., Caballero, M.,
1031 Goguitchaichvili, A., Aguilar, B., Chagué-Goff, C., Goff, J., Ruiz-Fernández, A.-C., Ortiz, M.,
1032 Nava, H., Bautista, F., Lopez, G.I., Quintana, P., 2012. Extreme wave deposits on the Pacific
1033 coast of Mexico: Tsunamis or storms? — A multi-proxy approach. *Geomorphology* 139–140,
1034 360–371. <https://doi.org/10.1016/j.geomorph.2011.11.002>

1035 Roy, P.D., Caballero, M., Lozano, R., Ortega, B., Lozano, S., Pi, T., Israde, I., Morton, O., 2010.
1036 Geochemical record of Late Quaternary paleoclimate from lacustrine sediments of paleo-lake
1037 San Felipe, western Sonora Desert, Mexico. *Journal of South American Earth Sciences* 29,
1038 586–596. <https://doi.org/10.1016/j.jsames.2009.11.009>

1039 Sabatier, P., Dezileau, L., Briquieu, L., Colin, C., Siani, G., 2010. Paleostorm events revealed by clay
1040 minerals and geochemistry in coastal lagoon: a study case of Pierre Blanche (NW
1041 Mediterranean Sea). *Sedimentary Geology* 228, 205–217.

1042 Sabatier, P., Dezileau, L., Colin, C., Briquieu, L., Bouchette, F., Martinez, P., Siani, G., Raynal, O., Von
1043 Grafenstein, U., 2012. 7000 years of paleostorm activity in the NW Mediterranean Sea in
1044 response to Holocene climate events. *Quaternary Research* 77, 1–11.
1045 <https://doi.org/10.1016/j.yqres.2011.09.002>

1046 Sallenger, A.H., 2000. Storm Impact Scale for Barrier Islands. *Journal of Coastal Research* 16, 890–
1047 895.

1048 Santisteban, J.I., Mediavilla, R., López-Pamo, E., Dabrio, C.J., Zapata, M.B.R., García, M.J.G., Castaño,
1049 S., Martínez-Alfaro, P.E., 2004. Loss on ignition: a qualitative or quantitative method for
1050 organic matter and carbonate mineral content in sediments? *Journal of Paleolimnology* 32,
1051 287–299. <https://doi.org/10.1023/B:JOPL.0000042999.30131.5b>

1052 Sarrazin, J.-L., 2012. « Vimers de mer » et sociétés littorales entre Loire et Gironde (XIVe-XVIe siècle).
1053 *Norois* n° 222, 91–102.

- 1054 Sarrazin, J.-L., 2005. Le paysage salicole de l'île de Bouin à la fin du Moyen Âge, in: Chauvaud, F.,
1055 Péret, J. (Eds.), *Terres Marines, Histoire*. Presses universitaires de Rennes, Rennes, pp. 57–67.
- 1056 Sauzeau, T., 2014. L'histoire, les tempêtes et la prospective littorale face aux changements
1057 climatiques, in: Laget, F., Vrignon, A. (Eds.), *S'adapter à La Mer : L'homme, La Mer et Le*
1058 *Littoral Du Moyen Âge à Nos Jours, Enquêtes et Documents*. Presses universitaires de
1059 Rennes, Rennes, pp. 71–86.
- 1060 Scheffers, A., Engel, M., Scheffers, S., Squire, P., Kelletat, D., 2012. Beach ridge systems – archives for
1061 Holocene coastal events? *Progress in Physical Geography: Earth and Environment* 36, 5–37.
1062 <https://doi.org/10.1177/0309133311419549>
- 1063 Scheffers, A., Kelletat, D., 2003. Sedimentologic and geomorphologic tsunami imprints worldwide—a
1064 review. *Earth-Science Reviews* 63, 83–92. [https://doi.org/10.1016/S0012-8252\(03\)00018-7](https://doi.org/10.1016/S0012-8252(03)00018-7)
- 1065 Scileppi, E., Donnelly, J.P., 2007. Sedimentary evidence of hurricane strikes in western Long Island,
1066 New York. *Geochemistry, Geophysics, Geosystems* 8, 25.
1067 <https://doi.org/10.1029/2006GC001463>
- 1068 Scoffin, T.P., 1993. The geological effects of hurricanes on coral reefs and the interpretation of storm
1069 deposits. *Coral Reefs* 12, 203–221. <https://doi.org/10.1007/BF00334480>
- 1070 Scott, D.B., Collins, E.S., Gayes, P.T., Wright, E., 2003. Records of prehistoric hurricanes on the South
1071 Carolina coast based on micropaleontological and sedimentological evidence, with
1072 comparison to other Atlantic Coast records. *GSA Bulletin* 115, 1027–1039.
1073 <https://doi.org/10.1130/B25011.1>
- 1074 Shimozono, T., Sato, S., 2016. Coastal vulnerability analysis during tsunami-induced levee overflow
1075 and breaching by a high-resolution flood model. *Coastal Engineering* 107, 116–126.
1076 <https://doi.org/10.1016/j.coastaleng.2015.10.007>
- 1077 Sorrel, P., Tessier, B., Demory, F., Delsinne, N., Mouazé, D., 2009. Evidence for millennial-scale
1078 climatic events in the sedimentary infilling of a macrotidal estuarine system, the Seine
1079 estuary (NW France). *Quaternary Science Reviews* 28, 499–516.
1080 <https://doi.org/10.1016/j.quascirev.2008.11.009>
- 1081 Spencer, C.D., Plater, A.J., Long, A.J., 1998. Rapid coastal change during the mid- to late Holocene:
1082 the record of barrier estuary sedimentation in the Romney Marsh region, southeast
1083 England. *The Holocene* 8, 143–163. <https://doi.org/10.1191/095968398673197622>
- 1084 Stager, J.C., Cumming, B.F., Laird, K.R., Garrigan-Piela, A., Pederson, N., Wiltse, B., Lane, C.S., Nester,
1085 J., Ruzmaikin, A., 2017. A 1600-year diatom record of hydroclimate variability from Wolf
1086 Lake, New York. *The Holocene* 27, 246–257. <https://doi.org/10.1177/0959683616658527>
- 1087 Steers, J.A., Stoddart, D.R., Bayliss-Smith, T.P., Spencer, T., Durbidge, P.M., 1979. The Storm Surge of
1088 11 January 1978 on the East Coast of England. *The Geographical Journal* 145, 192–205.
1089 <https://doi.org/10.2307/634386>
- 1090 Stewart, H., Bradwell, T., Bullard, J., Davies, S.J., Golledge, N., McCulloch, R.D., 2017. 8000 years of
1091 North Atlantic storminess reconstructed from a Scottish peat record: implications for
1092 Holocene atmospheric circulation patterns in Western Europe. *Journal of Quaternary Science*
1093 32, 1075–1084. <https://doi.org/10.1002/jqs.2983>
- 1094 Stockdon, H.F., Holman, R.A., Howd, P.A., Sallenger, A.H., 2006. Empirical parameterization of setup,
1095 swash, and runup. *Coastal Engineering* 53, 573–588.
1096 <https://doi.org/10.1016/j.coastaleng.2005.12.005>
- 1097 Suanez, S., Fichaut, B., Magne, R., 2009. Cliff-top storm deposits on Banneg Island, Brittany, France:
1098 Effects of giant waves in the Eastern Atlantic Ocean. *Sedimentary Geology* 220, 12–28.
1099 <https://doi.org/10.1016/j.sedgeo.2009.06.004>
- 1100 Thompson, T.A., Baedke, S.J., 1995. Beach-ridge development in Lake Michigan: shoreline behavior in
1101 response to quasi-periodic lake-level events. *Marine Geology* 129, 163–174.
1102 [https://doi.org/10.1016/0025-3227\(95\)00110-7](https://doi.org/10.1016/0025-3227(95)00110-7)
- 1103 Tisdall, E.W., McCulloch, R.D., Sanderson, D.C.W., Simpson, I.A., Woodward, N.L., 2013. Living with
1104 sand: A record of landscape change and storminess during the Bronze and Iron Ages Orkney,
1105 Scotland. *Quaternary International, Geoarchaeology: a toolbox of approaches applied in a*

1106 multidisciplinary research discipline 308–309, 205–215.
1107 <https://doi.org/10.1016/j.quaint.2013.05.016>

1108 Trouet, V., Scourse, J.D., Raible, C.C., 2012. North Atlantic storminess and Atlantic Meridional
1109 Overturning Circulation during the last Millennium: Reconciling contradictory proxy records
1110 of NAO variability. *Global and Planetary Change* 84–85, 48–55.
1111 <https://doi.org/10.1016/j.gloplacha.2011.10.003>

1112 Ulbrich, U., Christoph, M., 1999. A shift of the NAO and increasing storm track activity over Europe
1113 due to anthropogenic greenhouse gas forcing. *Climate Dynamics* 15, 551–559.
1114 <https://doi.org/10.1007/s003820050299>

1115 Vallve, M.B., Martin-Vide, J., 1998. Secular Climatic Oscillations as Indicated by Catastrophic Floods in
1116 the Spanish Mediterranean Coastal Area (14th–19th Centuries). *Climatic Change* 38, 473–
1117 491. <https://doi.org/10.1023/A:1005343828552>

1118 Van Vliet Lanoe, B., Goslin, J., Hallégouet, B., Hénaff, A., Delacourt, C., Fernane, A., Franzetti, M., Le
1119 Cornec, E., Le Roy, P., Pénaud, A., 2014. Middle- to late-Holocene storminess in Brittany (NW
1120 France): Part I - morphological impact and stratigraphical record. *Holocene* 24, 413–433.
1121 <https://doi.org/10.1177/0959683613519687>

1122 Van Vliet Lanoe, B., Lauer, T., Meurisse-Fort, M., Gosselin, G., Frechen, M., 2017. Late Holocene
1123 coastal dune activity along the Dover Strait, Northern France – Insights into Middle Ages and
1124 Little Ice Age coastal dynamics constrained by optically stimulated luminescence dating.
1125 *Zeitschrift der Deutschen Gesellschaft für Geowissenschaften* 168, 53–66.
1126 <https://doi.org/10.1127/zdgg/2016/0043>

1127 Vance, R.E., Mathewes, R.W., Clague, J.J., 1992. 7000 year record of lake-level change on the
1128 northern Great Plains: A high-resolution proxy of past climate. *Geology* 20, 879–882.
1129 [https://doi.org/10.1130/0091-7613\(1992\)020<0879:YRQLLC>2.3.CO;2](https://doi.org/10.1130/0091-7613(1992)020<0879:YRQLLC>2.3.CO;2)

1130 Wanner, H., Solomina, O., Grosjean, M., Ritz, S.P., Jetel, M., 2011. Structure and origin of Holocene
1131 cold events. *Quaternary Science Reviews* 30, 3109–3123.
1132 <https://doi.org/10.1016/j.quascirev.2011.07.010>

1133 Wassmer, P., Schneider, J.-L., Fonfrège, A.-V., Lavigne, F., Paris, R., Gomez, C., 2010. Use of
1134 anisotropy of magnetic susceptibility (AMS) in the study of tsunami deposits: Application to
1135 the 2004 deposits on the eastern coast of Banda Aceh, North Sumatra, Indonesia. *Marine*
1136 *Geology* 275, 255–272. <https://doi.org/10.1016/j.margeo.2010.06.007>

1137 Weisse, R., von Storch, H., Callies, U., Chrastansky, A., Feser, F., Grabemann, I., Günther, H., Pluess,
1138 A., Stoye, T., Tellkamp, J., Winterfeldt, J., Woth, K., 2009. Regional Meteorological–Marine
1139 Reanalyses and Climate Change Projections. *Bulletin of the American Meteorological Society*
1140 90, 849–860. <https://doi.org/10.1175/2008BAMS2713.1>

1141 Williams, D.M., Hall, A.M., 2004. Cliff-top megaclast deposits of Ireland, a record of extreme waves in
1142 the North Atlantic—storms or tsunamis? *Marine Geology* 206, 101–117.
1143 <https://doi.org/10.1016/j.margeo.2004.02.002>

1144 Williams, H., Choowong, M., Phantuwongraj, S., Surakietchai, P., Thongkhao, T., Kongsan, S., Simon,
1145 E., 2015. Geologic Records of Holocene Typhoon Strikes on the Gulf of Thailand Coast.
1146 *Marine Geology* 372, 66–78. <https://doi.org/10.1016/j.margeo.2015.12.014>

1147 Wilson, P., McGourty, J., Bateman, M.D., 2004. Mid-to late-Holocene coastal dune event stratigraphy
1148 for the north coast of Northern Ireland. *The Holocene* 14, 406–416.
1149 <https://doi.org/10.1191/0959683604hl716rp>

1150 Woodruff, J.D., Donnelly, J.P., Okusu, A., 2009. Exploring typhoon variability over the mid-to-late
1151 Holocene: evidence of extreme coastal flooding from Kamikoshiki, Japan. *Quaternary Science*
1152 *Reviews, Quaternary Ice Sheet-Ocean Interactions and Landscape Responses* 28, 1774–1785.
1153 <https://doi.org/10.1016/j.quascirev.2009.02.005>

1154 Xiong, H., Huang, G., Fu, S., Qian, P., 2018. Progress in the Study of Coastal Storm Deposits. *Ocean*
1155 *Science Journal* 53, 149–164. <https://doi.org/10.1007/s12601-018-0019-x>

1156 Yim, J., Kwon, B.-O., Nam, J., Hwang, J.H., Choi, K., Khim, J.S., 2018. Analysis of forty years long
1157 changes in coastal land use and land cover of the Yellow Sea: The gains or losses in

1158 ecosystem services. *Environmental Pollution* 241, 74–84.
1159 <https://doi.org/10.1016/j.envpol.2018.05.058>
1160 Yu, K.-F., Zhao, J.-X., Shi, Q., Meng, Q.-S., 2009. Reconstruction of storm/tsunami records over the
1161 last 4000 years using transported coral blocks and lagoon sediments in the southern South
1162 China Sea. *Quaternary International* 195, 128–137.
1163 <https://doi.org/10.1016/j.quaint.2008.05.004>
1164 Yuan, F., Koran, M.R., Valdez, A., 2013. Late Glacial and Holocene record of climatic change in the
1165 southern Rocky Mountains from sediments in San Luis Lake, Colorado, USA.
1166 *Palaeogeography, Palaeoclimatology, Palaeoecology* 392, 146–160.
1167 <https://doi.org/10.1016/j.palaeo.2013.09.016>
1168 Zhu, Z., Feinberg, J.M., Xie, S., Bourne, M.D., Huang, C., Hu, C., Cheng, H., 2017. Holocene ENSO-
1169 related cyclic storms recorded by magnetic minerals in speleothems of central China.
1170 *Proceedings of the National Academy of Sciences* 114, 852–857.
1171 <https://doi.org/10.1073/pnas.1610930114>
1172

PRE-PRINT

1173 Figure 1. Coastal flooding parameters and the three overwash mechanisms

1174 Figure 2. Presentation of the two marine deposit scenarios in a coastal marsh during an
1175 extreme event

1176 Figure 3. Presentation of the three different timescales

1177 Figure 4. Construction of the three methodologies presented at the three different timescales

1178 Figure 5. Presentation of a study conducted with the long timescale method in Yeu island,
1179 from Pouzet et al. (2018a), modified

1180 Figure 6. Presentation of a study conducted with the meso timescale method in the Petite mer
1181 de Gâvres, from Pouzet (2018), modified

1182 Figure 7. Presentation of a study conducted with the sort timescale method in the Traicts du
1183 Croisic, from Pouzet et al. (2019), modified

1184 Figure 8. Synthesis of the method used at the three different timescales for the detection of
1185 past storm with sedimentological analyses

1186

1187

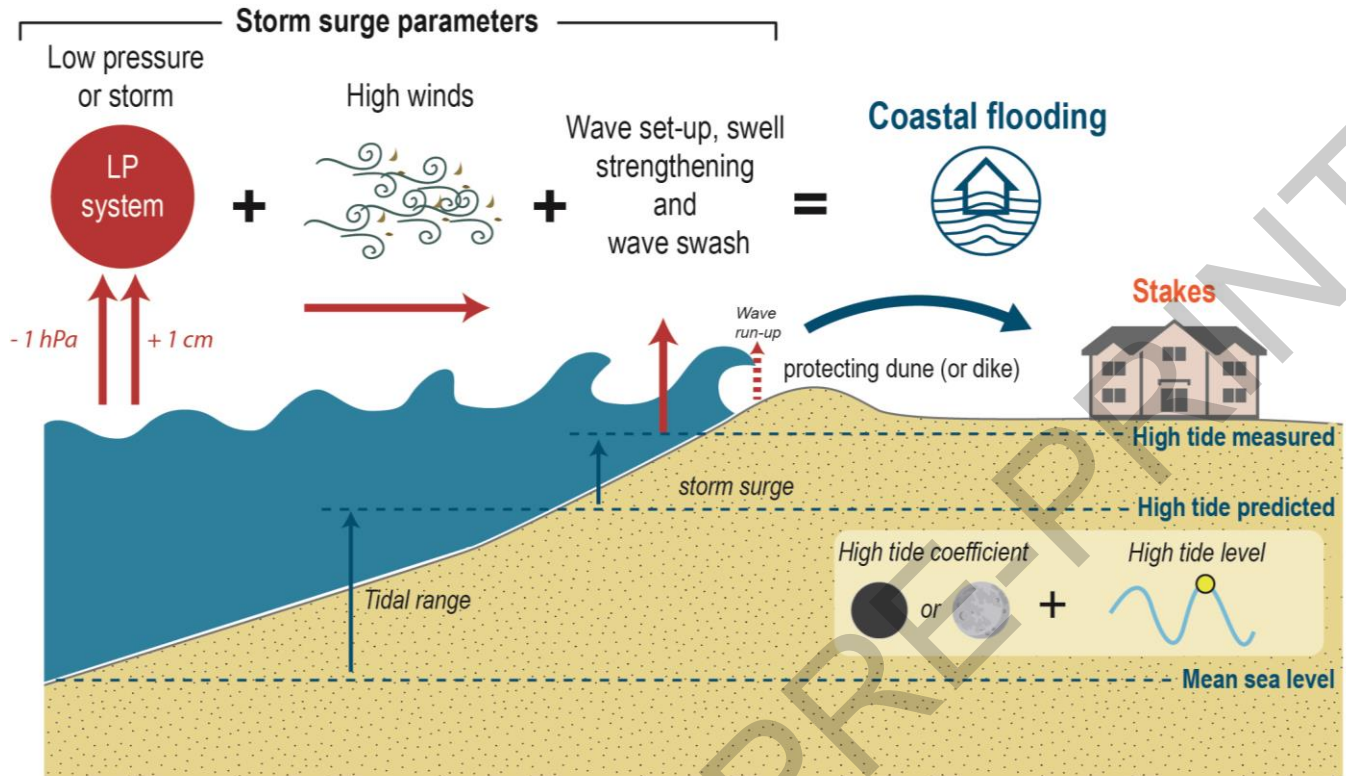
1188

1189

1190

1191

1192



A - Overflowing



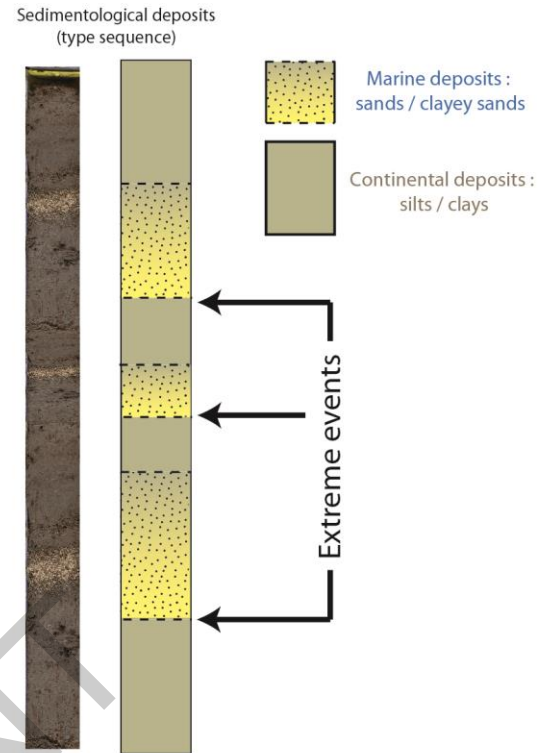
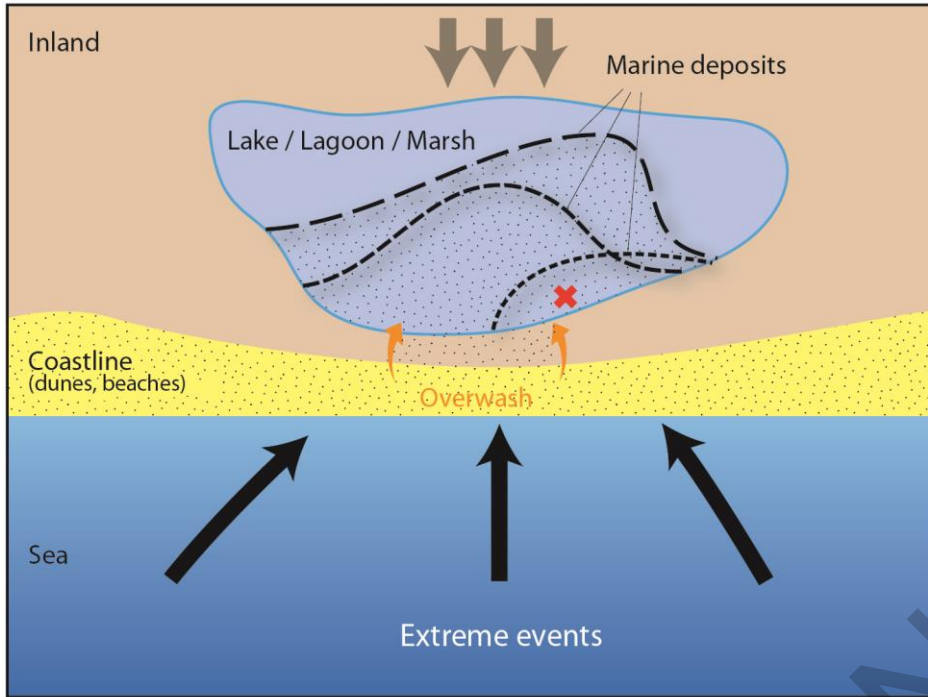
B - Overtopping



C - Breach

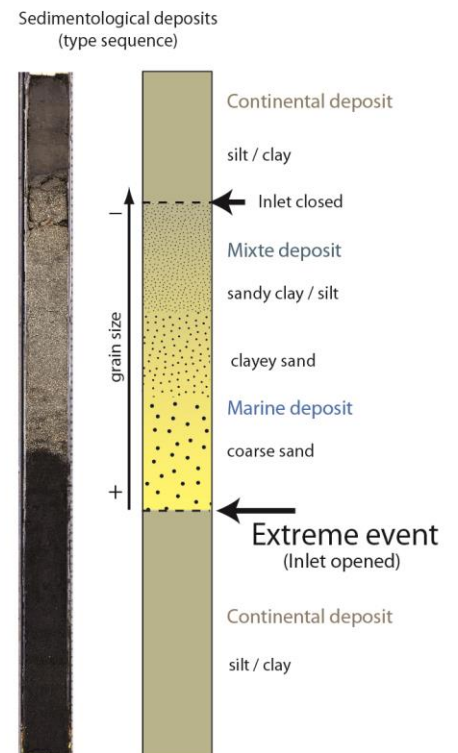
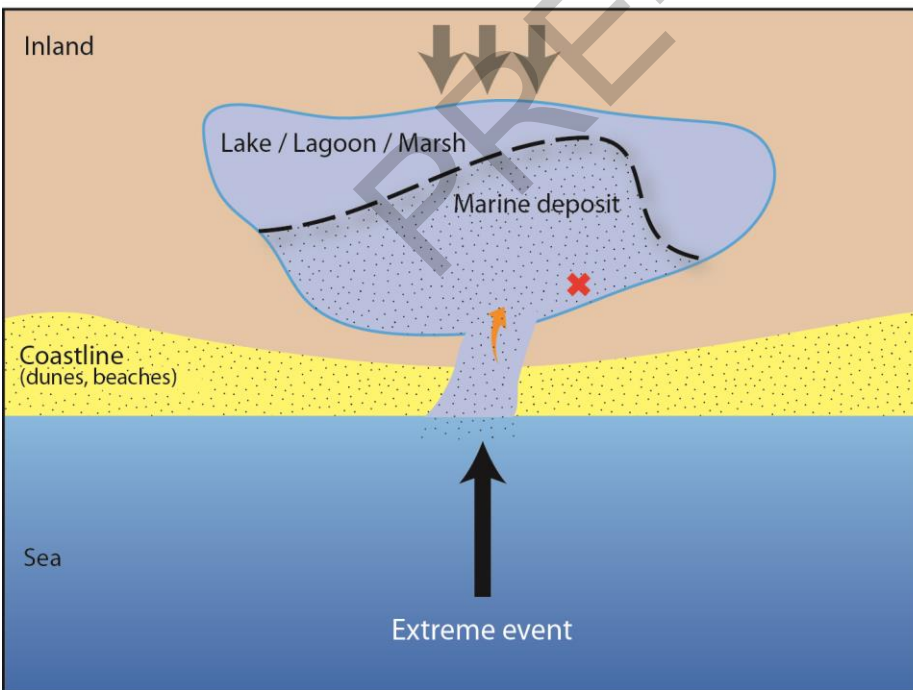


A. Overflowing or overtopping scenarios

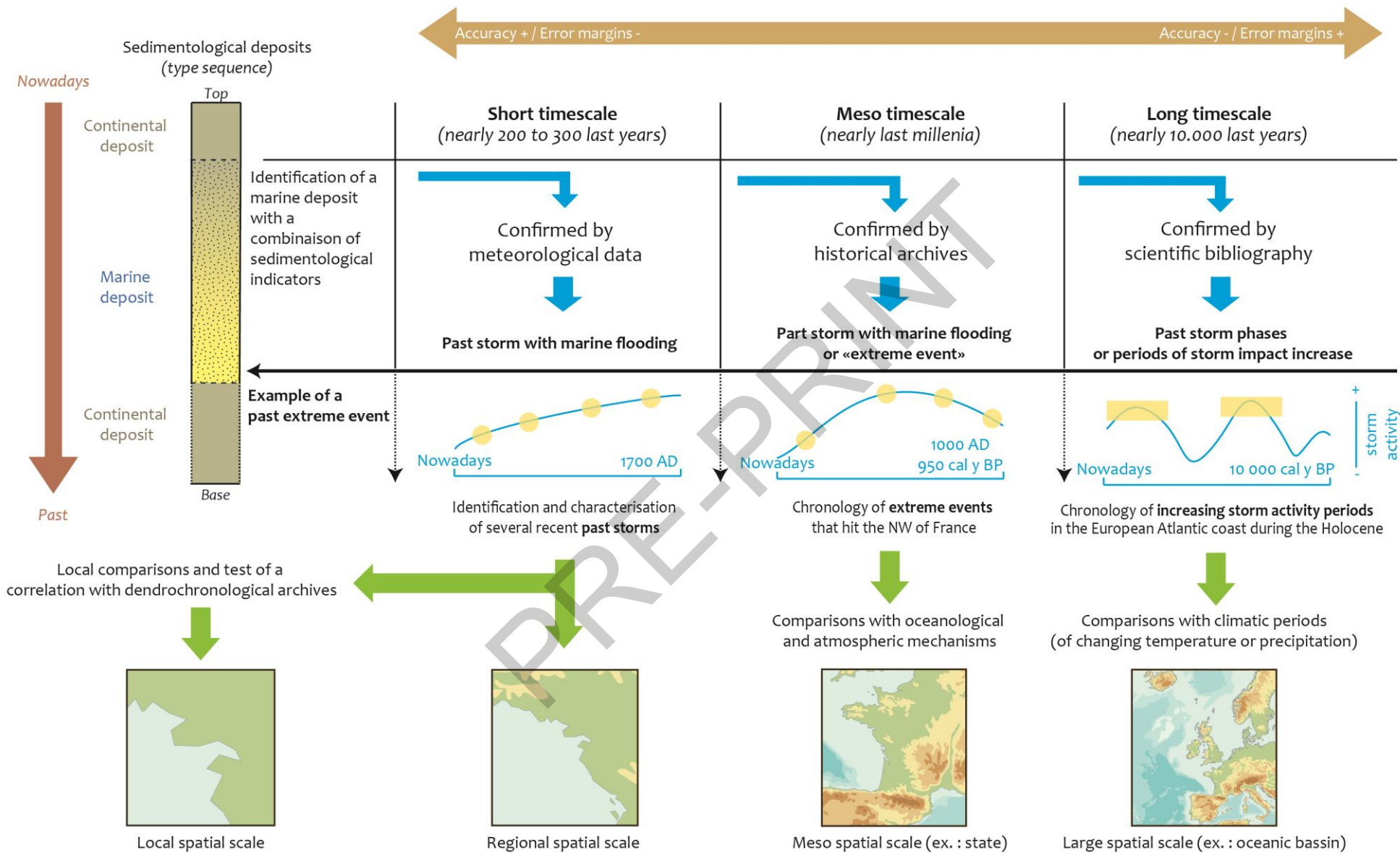


Singular transport of marine sediments by high winds and waves due to intense marine and atmospheric conditions
 Classic continental sedimentary filling
 Core extracted (once the marsh stabilized)

B. Breach scenario



Singular transport of marine sediments after a breach due to intense marine and atmospheric conditions
 Classic continental sedimentary filling
 Core extracted (once the marsh closed)

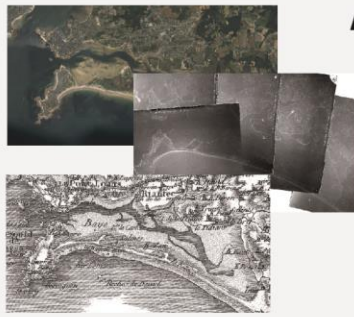


Ai. Selection of the study site

GIS : Analysis of ancient maps and photographs

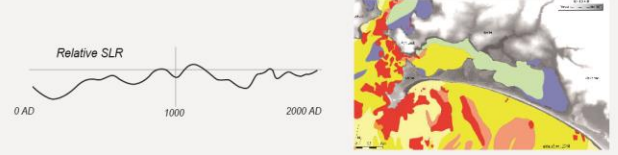
Reliability for washover detection :

- Back barrier environment
- Non anthropised
- Hit by storms



Aii. Analyse of the study site

- Geomorphology of the coast with elevation data
- Sedimentological map of the site
- Study of sea level rise, tidal and wave regimes
- Study of local storm dynamics and tsunami history



Long timescale

Ancient back-barrier environment, sealed coastal/salt marshes, ancient lakes, peat bogs,...



Meso timescale

B. Fieldwork

Back barrier lowland areas



Short timescale



«Schorre» environment of the back barrier lowland area

«Wet foreshore» environment of the back barrier lowland area



Compact sediments
Vibracore corer
Higher depths



Wet sediments
Beeker corer
One section of 1 - 1.5m depth

C. Sedimentological analyses

q.i : How to identify a marine layer and differentiate it from traditional lagoon, marsh or lake facies ?

Basic methods :
- Log and photography,
- Grain-size,
- Geochemistry,
- Radiography



Other possibilities : Pollens - Foraminifera - Molluscan assemblages - Clay minerals,...

+ Other precise possibilities :
e.g. spectrophotometry and
Magnetic Susceptibility (MS)



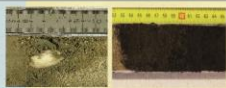
+ Information added for the paleoenvironmental reconstruction : Organic Matter (OM) curve steps
Loss on ignition or Dioxygen Burning (more accurate)



D. Isotopic dating

q.ii : When was the identified marine layer deposited in this coastal depositional environment ?

^{14}C : entire core
(shell, peat,
OM,...)



^{210}Pb / ^{137}Cs :
upper clayey
centimeters



E. Historical crossing

q.iii : How can we ensure that the marine layer comes from a natural hazard ?

Scientific bibliographic sources
of other environmental studies



Ancient
Historical
archives



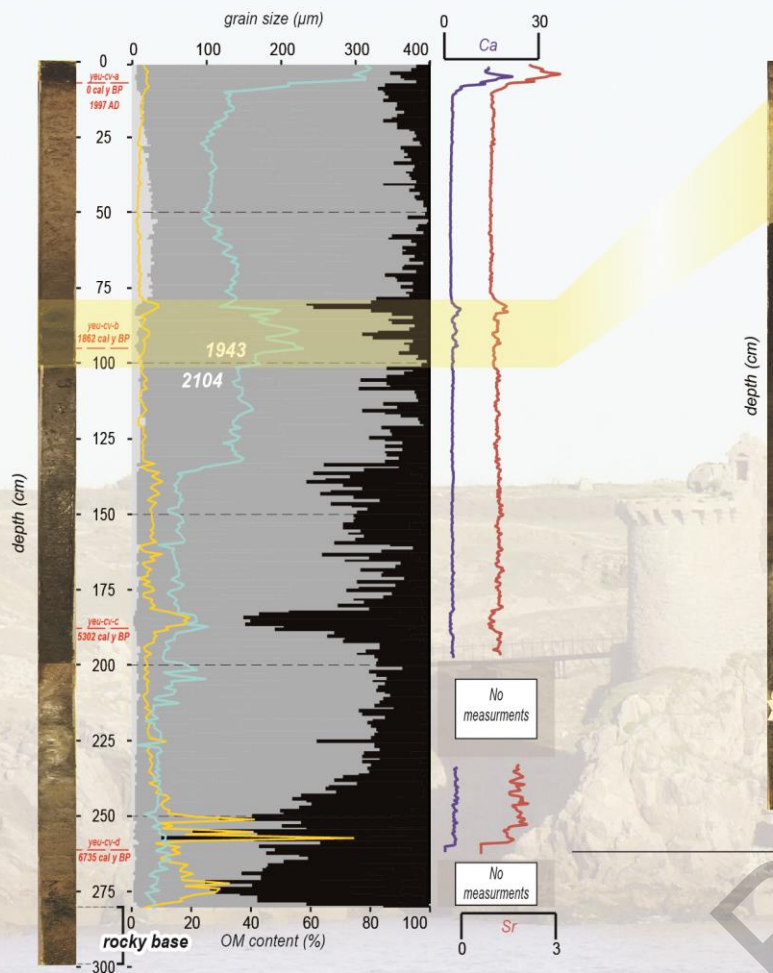
Newspaper records



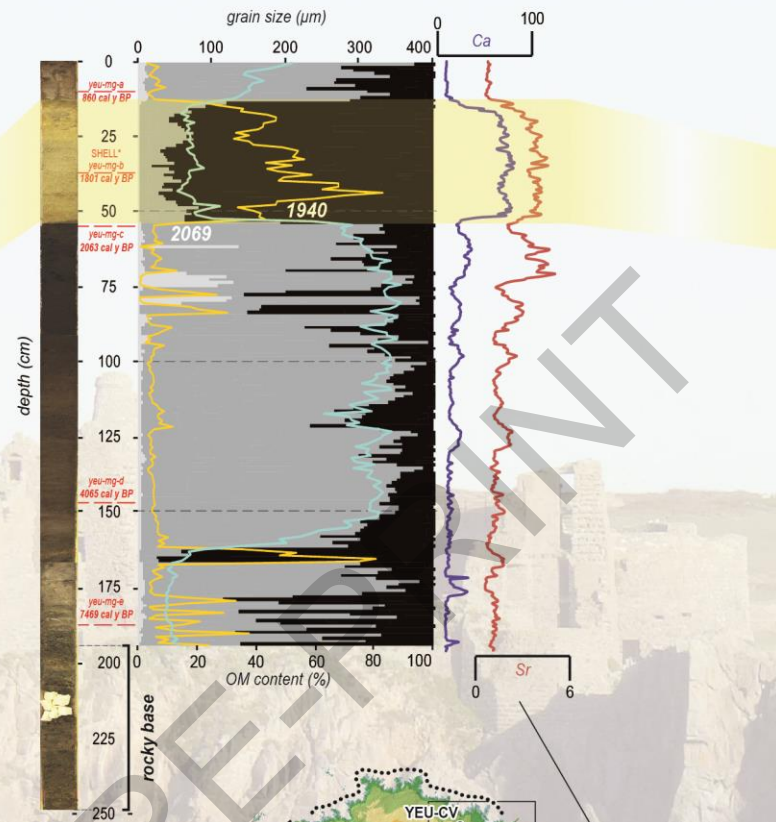
Meteorological,
oceanological,
and reanalysis
data



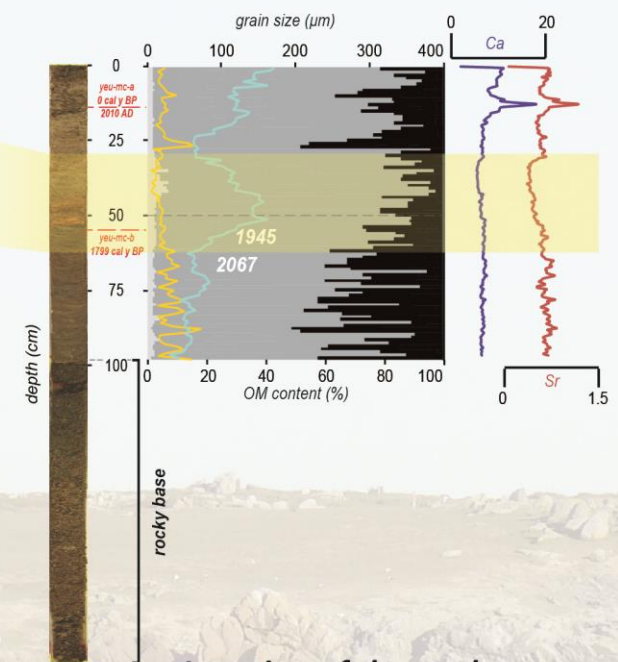
Coulée Verte



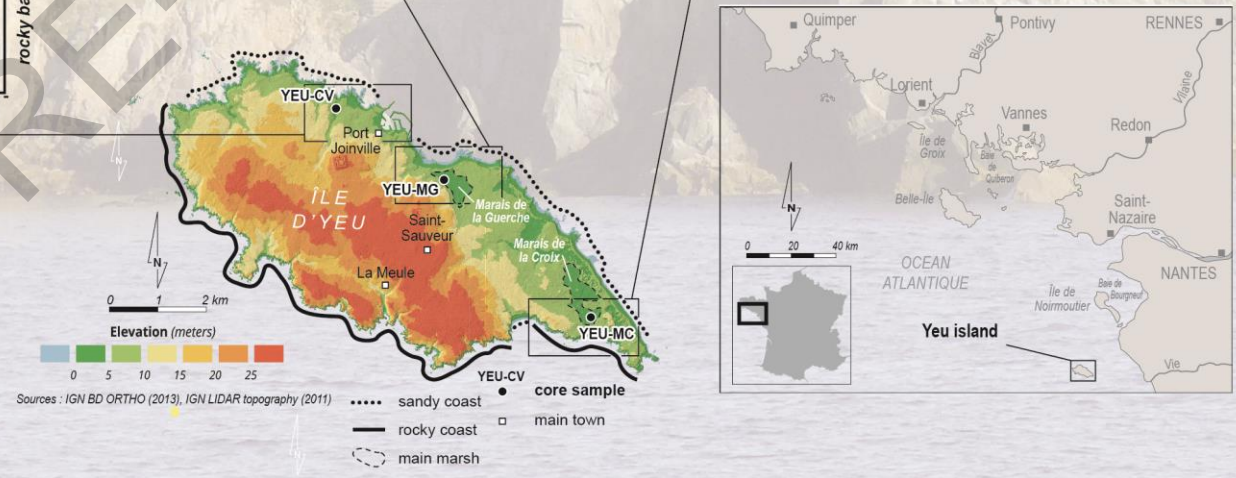
Marais de la Guerche



Marais de la Croix



Location of the study :



mean grain size (μm)	name of sample and measured Carbon-14 date
organic matter (%)	<i>Bitium reticulatum</i> shell dated, datation not preserved for age depth modelling
Sediment composition (%)	SHELL*
clay	date cal y BP of disturbance estimated with age depth modeling
silt	
sand	

